VYSOKÉ UČENÍ TECHNICKÉ V BRNĚ

BRNO UNIVERSITY OF TECHNOLOGY

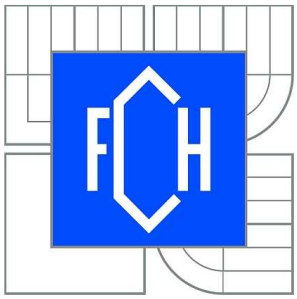

FAKULTA CHEMICKÁ
ÚSTAV CHEMIE MATERIÁLŮ

FACULTY OF CHEMISTRY
INSTITUTE OF MATERIALS SCIENCE

SYNTHESIS OF FOAMED BIOCERAMICS FOR POTENTIAL MEDICAL APPLICATIONS

SYNTÉZA PĚNOVÉ BIOKERAMIKY PRO POTENCIÁLNĚ LÉKAŘSKÉ APLIKACE

DIPLOMOVÁ PRÁCE
MASTER'S THESIS

AUTOR PRÁCE — Bc. PETR DOBOŠ
AUTHOR

VEDOUCÍ PRÁCE — doc. Dr. Ing. MARTIN PALOU
SUPERVISOR

BRNO 2012

Brno University of Technology
Faculty of Chemistry
Purkyňova 464/118, 61200 Brno 12

Master's thesis Assignment

Number of master's thesis:	**FCH-DIP0635/2011**	Academic year: **2011/2012**
Institute:	Institute of Materials Science	
Student:	**Bc. Petr Doboš**	
Study programme:	Chemistry, Technology and Properties of Materials (N2820)	
Study field:	Chemistry, Technology and Properties of Materials (2808T016)	
Head of thesis:	**doc. Dr. Ing. Martin Palou**	
Supervisors:		

Title of master's thesis:

Synthesis of foamed bioceramics for potential medical applications

Master's thesis assignment:

Preparation of porous materials by using foaming agents, study of microstructure, phase composition and bioactivity

Deadline for master's thesis delivery: 11.5.2012

Master's thesis is necessary to deliver to a secreatry of institute in three copies and in an electronic way to a head of master's thesis. This assignment is enclosure of master's thesis.

- -	- -	- -
Bc. Petr Doboš	doc. Dr. Ing. Martin Palou	prof. RNDr. Josef Jančář, CSc.
Student	Head of thesis	Head of institute

In Brno, 15.1.2012

- -
prof. Ing. Jaromír Havlica, DrSc.
Dean

ABSTRACT
The main aims of the diploma work were focused on the preparation of porous hydroxyapatite ceramics for potential biomedical applications. Hydroxyapatite slurries were synthesized by sol-gel and precipitation method. Then, the slurries were dried and calcinated at 1000 °C for phase control. These samples of HAP were analyzed by SEM, FTIR, and XRD. To prepare apatite porous ceramics, the slurries were foamed by polymeric sponge method and direct foaming method including (polymeric expancel and glass bubbles). The sintering temperature was established after 1 000 °C by sponge method and 1 200 °C by direct foaming.
The microstructure measurement by SEM and structure analysis by MIP of both porous hydroxyaptite indicates the regular porosity including macro, meso and micropores with different pore size distribution. The average size of pores prepared by sponge method is found between 1-5 µm with mono-dispersed porosity. The total porosity is 63.5 % with the total surface area 3.048 1 m/g. Porous hydroxyapatite prepared from expancel showed a poly-dispersed porosity with three main areas: 50–100 µm, 5–10 µm and the third one in range 0.5–1 µm, respectively. The total porosity is 67.6 % with total surface area 19.090 3 m/g. The bioactivity of both was tested in SBF for 7 days. It was found that in precipitation method was observed non-compact bioactive layer. The results were measered by SEM analysis.

ABSTRAKT
Cílem práce byla příprava porézních vzorků HAP pro potenciálně medicínské aplikace. HAP byl připraven metodou sol-gel a precipitační. Vzorky HAP byly podrobeny analýze FTIR, XRD, SEM. Takto připravený HAP byl napěněn pomocí houbové metody s jasně definovanými póry a pomocí polymerního a skleněného expanzelu s různou distribucí a velikostí pórů. U výsledných napěněných vzorků byla vyhodnocena mikrostruktura a povrchová analýza pomocí SEM, zjištěna porozita pomocí Hg porozimetru a sledována bioaktivita in *vitro* v SBF. Byly zjištěny jasně definované makro, mezo a mikro póry při různé distribuci. U houbové metody pomocí sol-gel došlo k vytvoření jasně definovaných a pravidelných pórů s monodisperzní porozitou. Dominantní velikost póru byla stanovena v rozmezí 1–5 µm. Celková porozita byla stanovena na 63,5 % s celkovým povrchem 3,048 1 m/g. Precipitační metodou s polymerním expanzelem došlo k polydisperznímu rozložení pórů s třemi hlavními fázemi v rozmezí: 50–100 µm, 5–10 µm a 0,5–1 µm. Celková porozita byla stanovena na 67,6 % s celkovým povrchem 19,090 3 m/g. Bioaktivita výsledných napěněných vzorků in *vitro* byla sledována po dobu 7 dnů v připraveném SBF. Při napěnění sol-gel houbovou metodou nevznikla výsledná bioaktivní vrstva. U precipitační metody napěněné pomocí polymerního expanzelu vznikla nepravidelná bioaktivní vrstva. Výsledky byly naměřeny pomocí SEM analýzy.

KEYWORDS
sol-gel method, hydroxyapatite, foaming agents, microstructure, bioactivity

KLÍČOVÁ SLOVA
sol-gel metoda, hydroxyaptit, pěnidla, mikrostruktura, bioativita

DOBOŠ, P. *Synthesis of foamed bioceramics for potential medical applications.* Brno: University of technology, Faculty of Chemistry, 2012, 58 p. Supervisor doc. Dr. Ing. Martin Palou.

DECLARATION

I declare that the diploma thesis has been worked out by myself and that all the quotations from the used literary sources are accurate and complete. The content of the diploma thesis is the property of the Faculty of Chemistry of Brno University of Technology and all commercial uses are allowed only if approved by both the supervisor and the dean of the Faculty of Chemistry, BUT.

.....
student's signature

ACKNOWLEDGEMENT

I would like to express my gratitude to doc. Dr. Ing. Martin Palou for his valuable guidance and overall encouragement.

Thank you

INTRODUCTION

The ceramics bioactive materials are used as they replace successfully advantages of biological tissues. The use of ceramics in medicine has increased significantly during the past decade and it is anticipated that the use of bioceramics will increase dramatically during the next years.

My study is focused on the preparation of porous bioceramics and the influence of porosity. The present study should be aimed to prepare of hydroxyapatite with different pore structure. Porosity is the most common factor that impact greatly the material properties. It changes significantly the mechanics and ossification properties of bioceramics. This matrix could be used as a scaffold for host tissue, cells growing and proliferation.

The first theoretical part is devoted to general definition, characterisation and classification of biomaterials. Next part is concerned with the uses of biomaterials in living tissue to replace or to repair damaged bones. The main section is devoted to hydroxyapatite preparations, manufacture, properties, mechanical strength and porosity. The last one should be written about ceramics foaming technique and porosity properties of ceramics, their types, behaviour and application.

The practical part is focusing on preparation and characterization of hydroxyapatite by sol-gel and precipitation method. Influence porosity by adding polymeric foaming agents in different preparation ways. The replica method using concretely by polymer sponge as a scaffold with clear porous diameter and direct foaming method with vary fillers. Finally, both of methods are compared and individually evaluated.

As the measuring devices will be using the Infrared spectroscopy for HAP slurry indicating, X-ray diffraction for quantitave analyse of ratio HAP/TCP and SEM analyse for studying porosity (distribution, pore sizes and surface region area) of each prepared samples. Our goal will be analysed the representative pores samples by Mercury Intrusion porosimetry (MIP) and studying bioactivity in SBF.

1. BIOMATERIALS

Material intended to interface with biological systems to evaluate treat, augment or replace any tissue, organ or function of the body. Biomaterials and grafts are widely used in clinical applications. Regardless of their composition or application, material used for body repair must meet both biofunctionality and biocompatibility [1].

Biocompatibility is defined as the ability of a material to perform with an appropriate host response in a specific application [1].

Biofunctionality concerns the ability of the implant to perform the purpose for which it was designated. These requirements are [1]:

- Mechanical properties (such as tensile strength, fracture toughness, fatigue strength, Young´s modulus)
- Physical properties (such as density or thermal expansion)
- Surface chemistry (such as degradation resistance, oxidation, corrosion or bone bonding ability)

The field of biomaterials is multidisciplinary, and the design of biomaterials requires the synergistic interaction of materials science, biological science, chemical science, medical science and mechanical science [2].

If we focus on functional artificial biomaterials, the choice has to be made among metals, polymers and ceramics. Each group exhibits some a priori advantages and drawbacks [3].

Over the last 30 years, ceramics, glasses and glass-ceramics for use in the medical field, which are grouped together and termed “bioceramics” [4]. Bioceramics, for instance, are the most biocompatible materials and can be obtained with biostable, bioactive or bioresorbable properties, but their main drawbacks are their hardness and fragility [3].

Metals exhibit problems of corrosion and toxicity, but their mechanical behaviour is optimum [3]. The implants made of these provide the strength and toughness [4]. For this reason, metals and metallic alloys are used in orthopedics, dentistry and other lead-bearing applications [2].

Polymers offer many possibilities depending on their chemical composition and structure (biodegradability degree, hydrophilic/hydrophobic ratio, toughness/flexibility, *etc.*), but very few have shown good bioactive properties (e.g. Poliactive) to ensure the implant osteo-integration [3]. The medical use of synthesis polymers also has a long history and the success of polymers in medicine can be exemplified by the application of PMMA and UHMWPE in total hip replacement [4].

Therefore, it is important to reach the best compromise possible, and it is quite usual to use the three types of materials in the same implant.These materials are known as Composites. This is the case of a total hip joint prosthesis which presents a metal beam, partially coated with a bioactive ceramic, while the head is made of an inert ceramic and the socket is made of polymer [3].

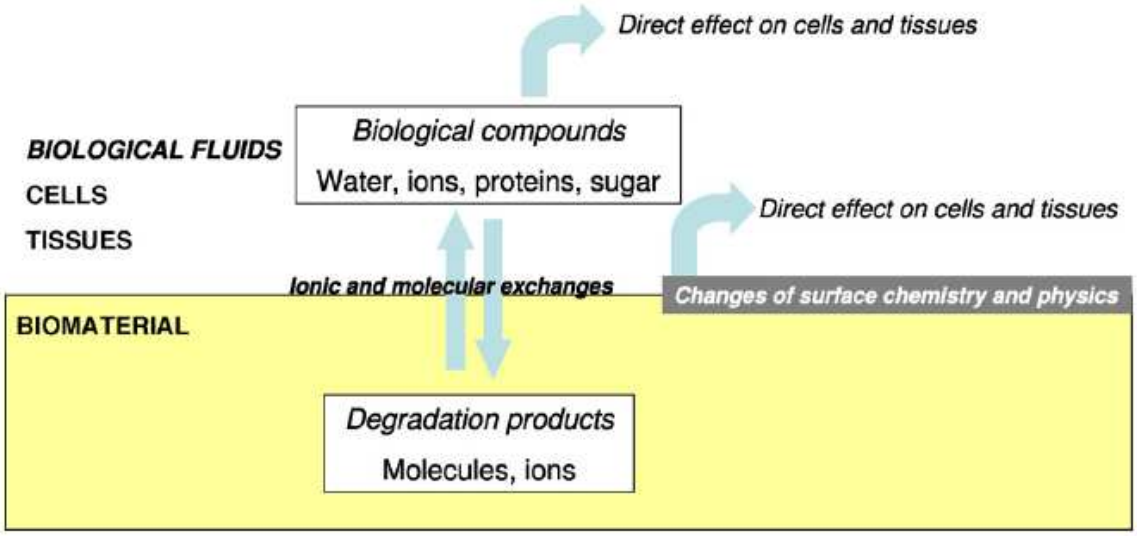

Fig. 1: Physico-chemistry of the biomaterial in contact with biological milieu [1].

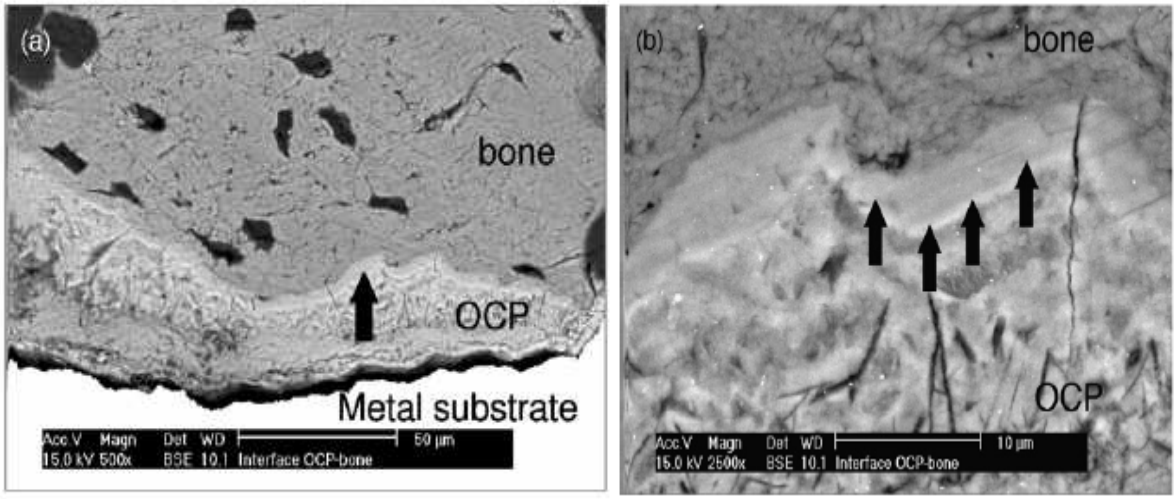

Fig. 2: Scattering electronic microscopy picture of an calcium phosphate coating (OCP) on a metallic porous scaffold implanted for 12 weeks in the femoral condyle at different magnification (scale bar (a) 50 µm and (b) 100 µm. Between the OCP and the newly formed bone, an interfacial phase (arrow) that can be attributed to superficial phase transformation is clearly visible [1].

1.1 Biomaterial generations

When a synthetic material is placed within the human body, tissue reacts towards the implant in a variety of ways depending on material types. The mechanism of tissue interaction (if any) depends on the tissue response to the implant surface. In general, there are three categories in which a biomaterial may be described in or classified into representing the tissue responses [5].

- First generation (Bioinert material)
- Second generation (Bioactive and resorbable)
- Third generation (Cell and gene-activating materials)

1.1.1 Bioinert material

The term bioinert refers to any material that once placed in the human body has minimal interaction with its surrounding tissue, examples of these are stainless steel, titanium, alumina, partially stabilised zirconia and ultra high molecular polyethylene. Generally, a fibrous capsule might form around bioinert implants hence its biofunctionality relies on tissue integration through the implant [5].

1.1.2 Bioactive and resorbable material

Bioactive refers to a material, which upon being placed within the human body direct interacts with the surrounding bone and in some cases, even soft tissue. This occurs through a time-dependent kinetic modification of the surface, triggered by their implantation within the living bone. Prime examples of these materials are synthetic hydroxyapatite (HAP), glass ceramic A-W and bio-glass [5].

Bioresorbable refers to a material that upon placement within the human body starts to dissolve (resorbed) and slowly replaced by advancing tissue (such as bone). Common examples of bioresorbable materials are tricalcium phosphate [$Ca_3(PO_4)_2$] and polylactic-polyglycolic acid copolymers. Calcium oxide, calcium carbonates are other common materials that have utilised during the last three decades [5].

1.2 Tissue engineering

Tissue engineering is a multidisciplinary field that applies the principles of biology and engineering to develop tissue substitutes. Currently, this is done by providing a porous scaffold which mimics the body´s own extracellular matrix onto which cells attach, migrate and growth. Materials used in tissue engineering as scaffold must be biocompatible, promote cell adhesion and growth. Over time, as cells produce their own matrix, the scaffold should degrade into non-toxic components which can be eliminated from the body. Several scaffolds have developed and tested. The most used natural material is collagen due to its non-antigenic, non-toxic, biocompatible, biodegradable, and bioresorbable properties. Collagen is obtained from renewable sources (mostly porcine and bovine skin) physiologically similar or almost identical to collagen in the human body [6].

The present target in synthetic biomaterials is to produce three-dimensional scaffolds with interconnected porosity so that cells can proliferate and form tissue in a similar way to the process in the human body. Macro-porous materials, where the pore sizes are in the order of microns are adequate as scaffolds for tissue engineering [3].

Materials such as calcium phosphate ceramics and calcium phosphate silica glass (or bioactive glasses) exhibit excellent bone-bonding properties that are related to the surface reactivity, via dissolution-precipitation mechanism [1].

2. CERAMICS

Ceramic is known as non-organic, non-metallic materials. Ceramic is typically crystalline in nature and are compounds formed between metallic and non-metallic elements.
The microstructure can be for ceramic entirely glassy, (glasses only), entirely crystalline or a combination of crystalline and glassy [51].
Typical properties for ceramics:

- hard and brittle
- high melting temperature
- wear resistance
- thermal and electrical insulators
- oxidation resistant
- chemically stable
- good aesthetic appearance

The thermal and chemical stability of ceramics, their high strength, wear resistance and durability makes ceramics good materials for inert implants. Ceramics are one of the few materials that are durable and stable enough to with stand the corrosive effect of body fluids. Ceramic is used for applications such as heart valves, orthopaedic implants and dental applications [51].

Ceramic has many wanted properties such as hardness, chemical stability and corrosion-resistivity, but they are brittle. Therefore combinations with polymers, metals and other ceramics have developed to achieve properties such as strength and elasticity. Ceramic coated, biocompatible metals have the strength and flexibility of metals and the abilities of ceramics to function with biological systems [51].

3. BIOCERAMICS

During the past 30–40 years there has been a major advance in the development of medical materials and this has been in the innovation of ceramic materials for skeletal repair and reconstruction. Bioceramic is now used in a number of different applications throughout the body. According to the type of bioceramics used and their interactions with the host tissue, they can be categorised [7]:

- Bioinert
- Bioactive
- Resorbable or non-resorbable

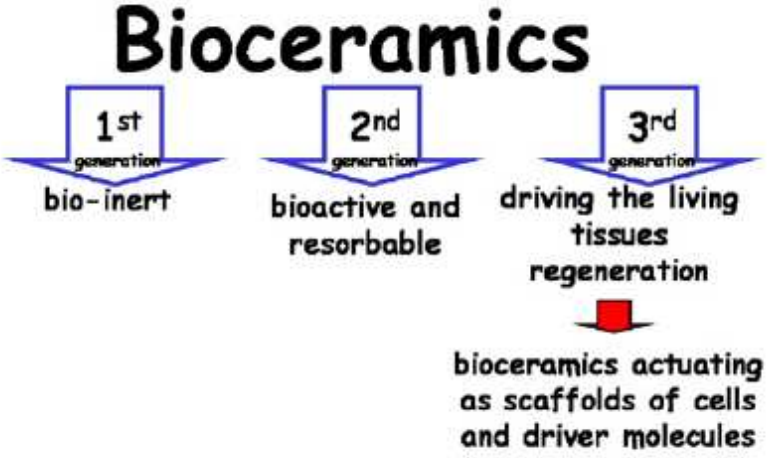

Fig. 3: Layout of the tree generations of bioceramics [3].

3.1 Bioceramic properties

Bioceramic has the advantage of being compatible with the human body environment. Their biocompatibility is a direct result of their chemical compositions which contain ions commonly found in the physiological environment (such as Ca^{2+}, K^{+}, Mg^{2+}, Na^{+}, etc.) and other ions showing very limited toxicity to body tissues (such as Al^{3+} and Zr^{4+}). Due to their excellent tribological properties and with their improved fracture toughness and reliability, structural ceramics such as alumina (high purity, polycrystalline, fine grained) and toughened zirconia (TZP) have used for femoral heads of total hip prostheses [4].

Elastic characteristics of the implant play a significant role. As an anisotropic material, cortical bone has a range of associated properties rather than a set of unique values: 7–30 GPa for Young´s modulus, 50–150 MPa for tensile strength, and 1–3 % for elongation at fracture [4].

When stiffer bioceramics stem is introduced into the canal, it shares the load and the carrying the capacity with bone. Originally, the load is carried by bone, but it is now carried by implant and bone. As a result, the bone is subjected to reduced stresses and hence stress shielded. For example: the upper part of the femur is receives fewer loads and down part of femur is overloaded. Decreasing in bone mass is known as bone resorption, may lead to the loosening of failure of the implant [8]. By decreasing the implant modulus of elasticity enhances implant to bone stress loading and can minimize bone atrophy due to stress shielding [8].

Materials	Tensile strength (MPa)	Elastic modulus (GPa)
Alloy		
Co-Cr alloys	655-1896	210-253
Co-Cr-Mo	600-1795	200-230
Ti-6Al-4V	960-970	110
Stainless steel 316 L	465-950	200
Polymers		
UHMWPE	21	1
PTFE	28	0.4
Ceramics		
Zirconia	820	220
Alumina	300	380

Fig. 4: Shows, mechanical properties of materials used in total hip replacement [8].

3.1.1 Zirconia and alumina material

The material is non-toxic and biologically inactive. Fibrous tissue capsule of a varying thickness forms around the material. Tissue response to immobilized inert bioceramics involves the formation of a very thin, several micrometres or less, fibrous membrane surrounding the implant material [9].

The nearly inert ceramics most used for surgical implants are alumina and zirconia.

Alumina ceramic is known with high-density and high purity (>99,5 %). Although some dental implants are single crystal sapphire, most Al_2O_3 devices are very fine-grained polycrystalline α-Al_2O_3 produced by pressing and sintering at temperatures ranging from 1 600 °C to 1 800 °C. This ability is used in load-bearing hip and knee prostheses and dental implants because of its combination of excellent corrosion resistance, good biocompatibility, high wear resistance and high strength. The outstanding fractional and wear properties are due to the material´s extremely low surface roughness and to their high surface energy which results in the fast and strong adsorption of biological molecules. However, it exhibits moderate fluxural strength and toughness. Alumina implants have used for various neurosurgical operations such as cranioplasty, maxillofacial surgery, eye prostheses consisting of a sapphire single crystal optical part *etc*.[9].

Zirconia ceramic have an advantage over alumina of higher fracture toughness and higher flexural strength and lower Young´s Modulus. The main problem to use zirconia for bearing surfaces are reported strength reduction with time in physiological fluids. The second is its wear properties and third is the potential radioactivity of material [8].

The deleterious martensitic transformation from tetragonal to monoclinic is well known. It can lead to increasing material volume by 5 % and friction result, reducing toughness and catastrophic fracture [9].

The phenomena of slow crack growth, static and cyclic fracture, low toughness, stress corrosion are used in high load bearing applications [9].

3.1.2 Bioglass

In the early 1970s, Hench reported that particular compositions with the Na_2O-CaO-P_2O_5-SiO_2 system with B_2O_3 and CaF_2 additions formed a strong, adherent bond with bone. The equilibrium phase diagram for Na_2O-CaO-SiO_2 shows a ternary eutectic near the 45S5 composition (the 45 representing 45 wt. % SiO_2, S being the network former and 5 representing the ratio of CaO to P_2O_5) [7].

The first and most well studied composition contains 45 % SiO_2, 24.5 % Na_2O, 24.4 % CaO and 6 % P_2O_5 all in wt.% [9].

Hench and his co-workers have studies a series of glasses with this four components system with a constant 6 % P_2O_5 content. This work is summarized in the ternary Si_2O-Na_2O-CaO diagram shown in Fig. 5. The figure establishes the bioactive-bonding-boundary of compositions [9].

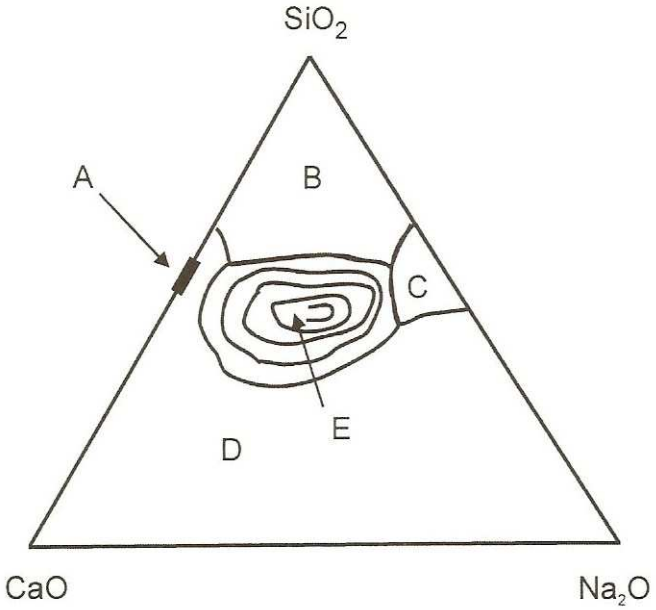

Fig. 5: Phase diagram highlight the chemical compound of bioglasess in area (A-E) with different biological and mechanical response [33].

In region A the glasses are bioactive and bond to bone. Glasses in region B behave as nearly inert materials and are encapsulated by non-adherent fibrous tissue when implanted. Compositions, in region C, are resorbed within 10 to 30 days in tissue. In region D the compositions are not technical practical and have not implanted. The boundary between region A and C depends upon the ratio of surface area of the glass to the effective solution volume of the tissue, as well as the glass composition. Partial substitution of CaO by CaF_2 does not significantly alter the bone-bonding behaviour [9].

Highly bioactive material, in 1991, Hench proposed an in *vivo* bioactivity index I_B**,** which is defined:

$$I_B = 100 / t_{50bb}, \qquad [1.1]$$

where t_{50bb} is the time required for more than 50 % of the interface to be bonded [7].

The rate of bonding and the strength and stability of the bond vary with the composition and microstructure of the bioactive materials. The reporting that for their particular formulation of bioactive glass, bone formed a rapid bond when the silica levels were in the range 42–53 %; glasses with 54–60 % silica required 2–4 weeks for bone to bond; and bone did not form a direct bond with glasses containing more than 60 % silica [7].

The primary advantage of bioactive glasses is their rapid rate of surface reaction which leads to fast tissue bonding. Their primary disadvantage is mechanical weakness and low fracture toughness due to an amorphous two dimensional glass network. Tensile bending strength of most of the compositions is in the range of 40–60 MPa, which make them unsuitable for load-bearing applications [9]. However, these glasses have an excellent field of application on the filling of small defects, where the rate of regeneration is the main concern, and where mechanical properties are just a secondary aspect.

3.1.3 Bioactive glass-ceramics

Kokubo *et al.* have developed a new glass-ceramic materials in Japan and they first reported the production and behaviour of A-W glass-ceramics in 1982.

Apatite-wollastonite (A-W) glass-ceramics became one of the most extensively studied glass-ceramics for use as a bone substitute. β-wollastonite and oxyfluoroapatite crystals in 50–100 nm size in a MgO-CaO-SiO_2 glassy matrix. A dense and homogeneous composite was obtained after heat treatment of the parent glass, which comprised [7]:

Table 1: The Composition contents of (A-W) glass-ceramics final products.[7].

β-Wollastonite	34 wt% ($CaO \cdot SiO_2$)	
Oxyfluoroapatite	38 wt% ($Ca_{10}(PO_4)_6(O,F_2)$)	
Glass	28 wt% (CaO, MgO, SiO_2)	24 wt% CaO
		17 wt% MgO
		59 wt% SiO_2

Apatite-wollastonite glass-ceramic is an assembly of small apatite particles effectively reinforced by wollastonite. The bending strength, fracture toughness and Young´s modulus of A-W glass-ceramic are the highest among bioactive glass and glass-ceramic, enabling it to be used in some major compression load bearing applications, such as vertebral prostheses, intervertebral spacers, spinal spacers and iliac crest replacement. It combines high bioactivity with suitable mechanical properties [7].

Table 2: Physical properties of A/W glass-ceramic [51].

Density (g/cm^{-3})	3.07
Bending strength (MPa)	215
Compressive strength (MPa)	1 080
Young´s Modulus (GPa)	118
Vickers Hardness (HV)	680
Fracture Toughness ($MPa^{1/2}$)	2.0
Slow crack growth, n	33

The physical properties of the glass-ceramics A/W are summarised in Table 2. The bending strength (215 MPa) of this glass-ceramic is almost twice that (115 MPa) of dense sintered HAP and even higher than the (160 MPa) of human cortical bone in an air environment. It is evident that the high bending strength of A/W glass-ceramic is due to the precipitation of the wollastonite as well as apatite. The wollastonite effectively prevents straight propagation of the cracks, causing them to turn or branch out. It is notable that the wollastonite exhibits such as reinforcing effect, even it is not in fibrous form [9].

The A/W shows a decrease in resistance (even if slighter than for other glass-ceramics or some bioglasses) and corrosion similar to the normal ceramics. In the body, the glass-ceramics A/W resists for more of 10 years to a continuous bending stress equal to 65 MPa, while bioglasses, other glass-ceramics and dense sintered HAP would survive to such stress only 1 minute. The A/W has a high bioactivity, attributable to its specific surface property [10].

3.2 Bioceramic applications

Bioceramics are produced in a variety of forms and phases and serve many different functions in repair of the body, which are summarized in Fig. 6. In many applications ceramics are used in the form of bulk materials of a specific shape, called implants, prostheses, or prosthetic devices. Bioceramics are also used to fill space while the natural repair processes restore function. In other situations the ceramic is used as a coating on a substrate, or as a second phase in a composite, combining the characteristics of both into a new material with enhanced mechanical and biochemical properties [9].

Bioceramics are made in many different phases. They can be single crystals (sapphire), polycrystalline (alumina or HAP), glasses (Bioglass®), glass-ceramics (A/W glass-ceramics), or composites (e.g. polyethylene-hydroxyapatite). The phase depends on the properties and function required. For example, single crystal sapphire is used as a dental implant because of its high strength. A/W glass-ceramic is used to replace vertebrae because it has high strength and bonds to bone. Boactive glasses have low strength but bond rapidly to bone so are used to augment the repair of bone defects [9].

Another important aspect of ceramics and glasses is their brittleness and consequently very low strength in tension. Therefore, their use is mostly limited to compressive loading conditions, such as those in an acetabular cup or a femoral head of a total hip joint replacement. Some applications do not require high loading, including hydroxyapatite for artificial bone and barium sulphate ($BaSO_4$) for bone cement [11].

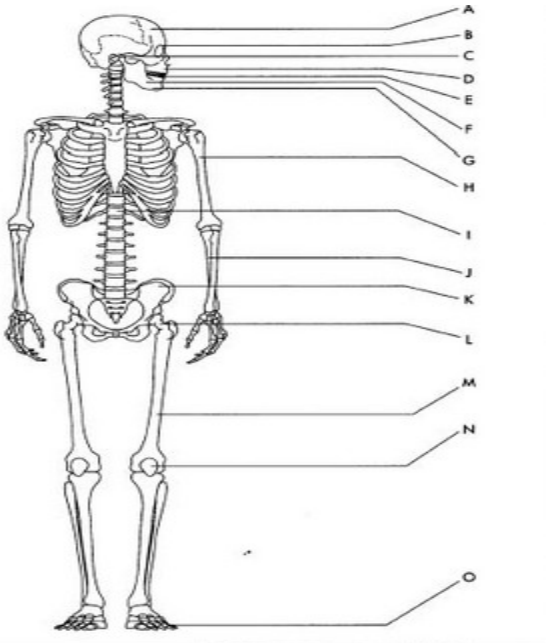

Fig. 6: Shows, where bioceramics may be used [12].

Bioceramic application A. Cranial repair, B. Eye lens, C. Otolaryngological implants, D. Facial reconstructions, E. Dental implants, F. Jaw augmentation, G. Periodontal pockets, H. Percutaneous devices, I. Spinal surgery, J. Iliac crest repair, K. Space fillers, L. Orthopedic support purposes, M. Orthopedic fillers, N. Artificial tendons, O. Joints [12].

4. HYDROXYAPATITE (HAP)

Hydroxyapatites (HAP) are naturally-occurring forms of calcium apatites, found in bone and teeth in the human body, with chemical formulae of $Ca_5(PO_4)_3(OH)$, but it is usually written as $Ca_{10}(PO_4)_6(OH)_2$ because the crystal unit cell is made up of two molecules. The crystal is hexagonal-shaped, and pure HAP powder is white in colour [13].

HAP is one of the most biocompatible ceramics because of its significant chemical and physical resemblance to the mineral constituents of human bones and teeth. It is a bioactive ceramics widely used as powders or in particulate forms in various bone repairs and as coatings for metallic prostheses to improve their biological properties. It has excellent biocompatibility, bioactivity and osteo-conduction properties. HAP is thermodynamically the most stable calcium phosphate ceramic compound nearest to the pH, temperature and composition of the physiological fluid [14].

4.1 HAP structure

HAP possesses a hexagonal structure with a P63/m space group and cell dimensions a=b=9,42 Å, and c=6,88 Å, where P63/m refers to a space group with a six-fold symmetry axis with a three-fold helix and a micro plane [14].

The crystal structure of HAP can accommodate substitutions by various other ions for the Ca^{2+}, $(PO_4)^{3-}$ and OH^- groups. The ionic substitutions can affect the lattice parameters, crystal morphology, crystallizations, solubility and thermal stability of HAP [7].

Natural apatites form a large number of aceptors with general formula $Me_{10}(XO_4)_6(Y)_2$, where Me contains big cations with coordination 7 and 9 (Ca, Sr, Ba, Pb, Mg). Anionic substitutions (X) occupied by atoms with tetraedric coordination (P, As, V, Si, S). The Y location is occupied by anions coordinated by three cations X (F^-, Cl^-, OH^-, O^-) [15].

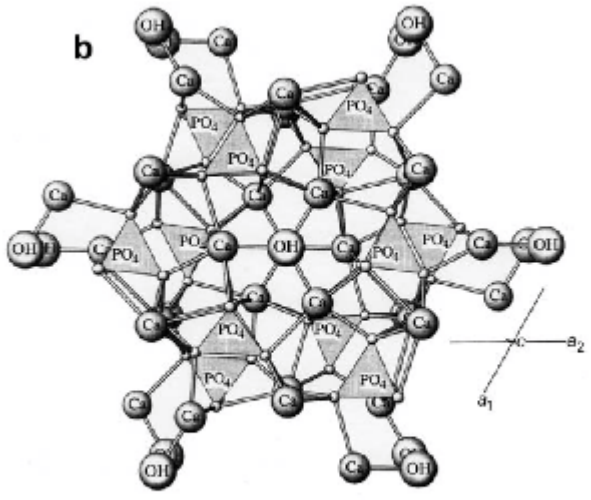

Fig. 7: The crystal structure of HAP [34].

4.2 HAP properties

Positive behaviour [13]:

- High biocompatibility and bioactivity due to its natural presence in the human body
- Non-toxic
- High structural stability
- High porosity–hence high surface area to volume ratio
- High adsorption

Negative behaviour:

- cannot replace bone in load bearing sites
- fragility
- low tensile strength

4.3 HAP applications

HAP has attracted widespread interesting the orthopaedic and dental fields. Recently, HAP has used for a variety of biomedical applications, including matrices for drug release control. Due to the chemical similarity between HAP and mineralized bone of human tissue, synthetic HAP exhibits strong affinity to host hard tissues. Formation of chemical bond with the host tissue offers HAP a greater advantage in clinical applications over most other bone substitutes, such as allograft or metallic implants [14]. HAP has used as a filler to replace amputated bone or as a coating to promote bone ingrowth into prosthetic implants due to the biocompatibility of the compound. It has also used to immobilise nuclear waste due to its high porosity [13].

4.4 HAP preparation

Several different HAP synthesis techniques have developed in recent years. These techniques include mechano-chemical synthesis and combustion preparation. Although, various types of wet chemistry techniques such as direct precipitation from aqueous solutions, electrochemical deposition, sol-gel procedures, hydrothermal synthesis, and emulsion or micro-emulsion routes are also widely used [16].

The solid state synthesis of HAP from oxide or inorganic salt powders usually requires extensive mechanical mixing and lengthy heat treatments at high temperatures. These processing conditions, however, do not allow facile control over micro-structure, grain size and grain size distribution in the resulting powders or shapes [17]. For this reason, the wet chemistry techniques for HAP are more applicable.

Extensive researches have carried out to prepare HAP in powder form, thin films and by using gel-casting techniques to obtain pieces with complex shapes [18].

4.4.1 Sol-gel methods

Sol-gel process for HAP preparing usually can produce fine-grain microstructure containing a mixture of nano-to-submicron crystals. These crystals can be better accepted by the host tissue [16].

The sol-gel product is characterized by nano-size dimension of the primary particles. This small domain is a very important parameter for improvement of the contact reaction and the stability at the artificial/natural bone interface. Moreover, the high reactivity of the sol-gel powder allows a reduction of processing temperature and any degradation phenomena occurring during sintering [16].

The major limitation of the sol-gel technique application is linked to the possible hydrolysis of phosphates and the high cost of the raw materials.

Most of the sol-gel processes require a strict pH control, vigorous agitation and a long time for hydrolysis. The gel formation has achieved without using any catalyst [16].

It has well demonstrated that the sol-gel process offers considerable advantages of good mixing of the starting materials and excellent chemical homogeneity of the product. Several sol-gel approaches starting from non-aqueous solutions of different precursors of calcium and phosphorus have used for the preparation of HAP powders. In these synthetic routes, e.g. calcium nitrate or different calcium alkoxides and 2-ethyl-hexyl phosphate, triethyl phosphate or orthophosphoric acid were used as calcium and phosphorus precursors, respectively. The major limitation for its applications was found to be very low solubility of the calcium alkoxides in the organic solvents and low reactivity of the phosphorus compounds. Effective control of stoichiometry due to the volatility of the phosphorous compounds used was also problematic [17].

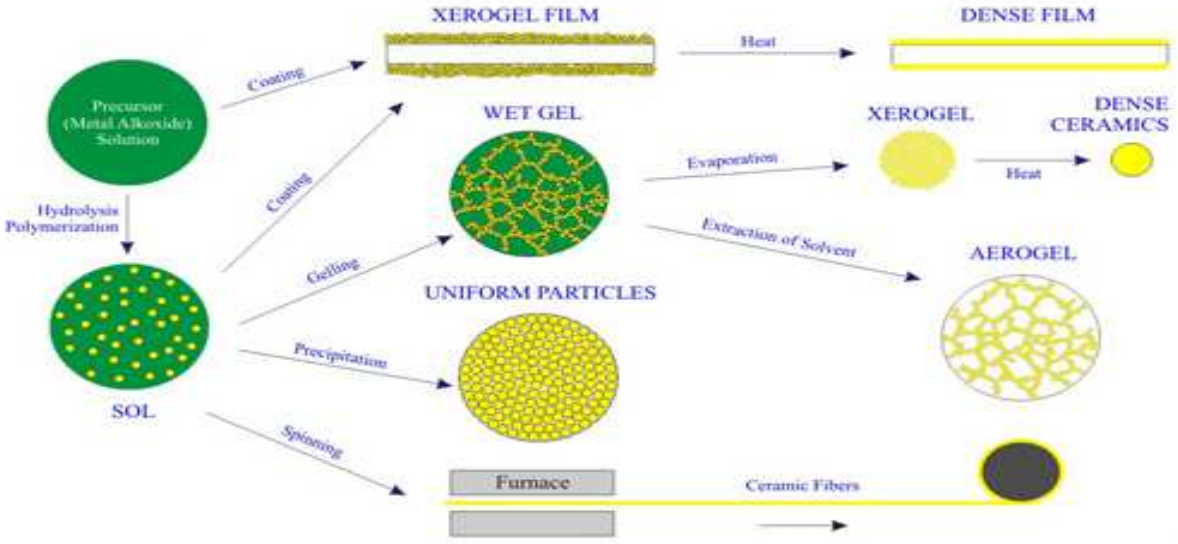

Fig. 8: Scheme the sol-gel technology to making various products [35].

4.4.1.1 Sol-gel processing

In the sol-gel process, the precursors (starting compounds) for preparation of a colloid consist of a metal or metalloid element surrounded by various ligands [19].

Metal alkoxides are popular precursors because they react readily with water. This reaction is called hydrolysis, because a hydroxyl ion becomes attached to the metal atom, as in the following reaction [19]:

$$M(OR)_n + n\ H_2O \rightarrow M(OH)_n + n\ ROH \quad [2.1]$$

$$Si(OR)_4 + H_2O \rightarrow HO–Si(OR)_3 + ROH \quad [2.2]$$

The R represents a proton or other ligand (if R is an alkyl, then OR is an alkoxy group), and ROH is an alcohol [19].

Depending on the amount of water and catalyst present, hydrolysis may go to complementation (so that all of the OR groups are replaced by OH),

$$Si(OR)_4 + 5\ H_2O \rightarrow Si(OH)_4 + 4\ ROH, \quad [2.3]$$

or stop while the metal is only partially hydrolysis, $Si(OR)_{4-n}(OH)_n$

Two partially hydrolysis molecules can link together in condensation reaction, such as

$$(OR)_3Si–OH + HO–Si(OR)_3 \rightarrow (OR)_3Si–O–Si(OR)_3 + H_2O \quad [2.4]$$

$$(OR)_3Si–OR + HO–Si(OR)_3 \rightarrow (OR)_3Si–O–Si(OR)_3 + ROH \quad [2.5]$$

By definition, condensation liberates a small molecule, such as water or alcohol. This type of reaction can continue to build larger and larger silicon containing molecules by the process of polymerization [19].

The formation of gels and gelation point is the time at which the last bond is formed that completes this giant molecule. Thus a gel is a substance that contains a continuous solid skeleton enclosing a continuous liquid phase. The continuity of the solid structure gives elasticity to the gel. Gels can also be formed from particulate sols, when attractive dispersion forces cause them to stick together in such a way as to form a network [19].

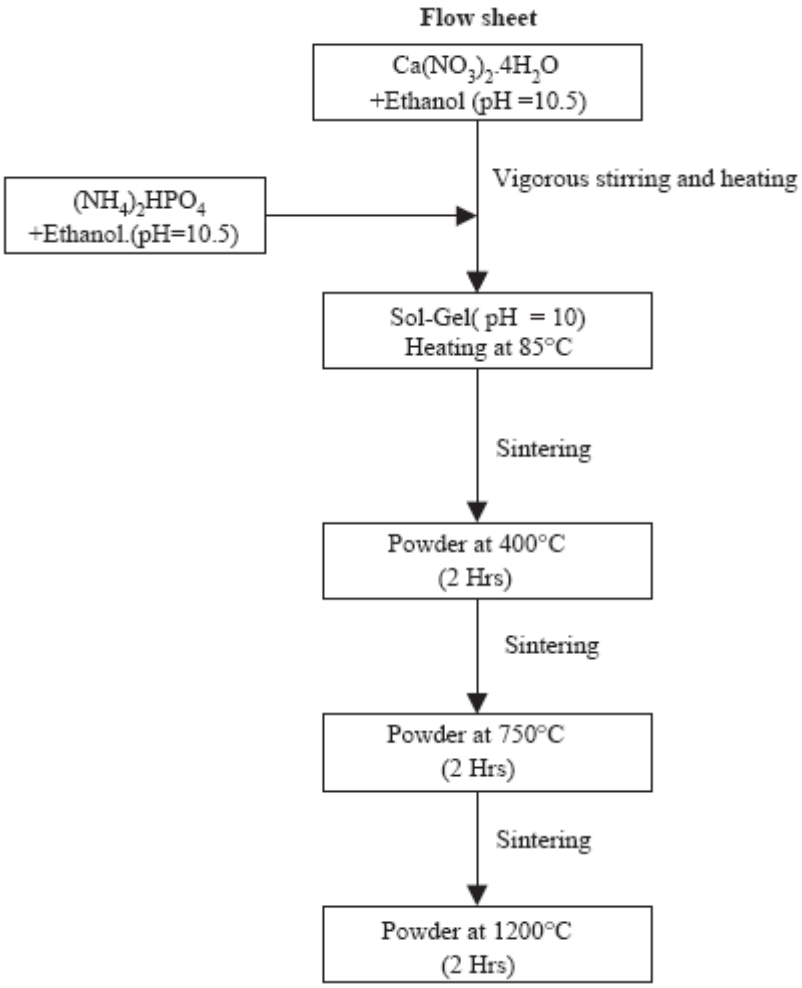

Fig. 9: Briefly characterization of individual preparation by sol-gel method [36].

5. TECHNOLOGY PRODUCTION

Several methods for HAP production are available, but mostly HAP is prepared by wet chemical reactions. It is a very versatile method that allows control of product properties such as morphology, size and reactivity, and therefore, it is a widely used method for the production of nanoparticles [20].

Commercial HAP samples exhibit a high degree of chemical and physical variability. Most of the commercially available HAP powders are calcium deficient hydroxyapatite (DHAP). Depending on the final application of HAP, other important properties that should be considered are purity, degree of crystallization, crystal and average particle size, heavy metal contamination, specific surface area, porosity and pores size distribution. For this reason, several companies cannot develop high quality products due to the lack of HAP properties reproducibility [20].

5.1 The NETmix® reactor

The technology of NETmix® (patent pending) has developed at the laboratory of Separation and Reaction Engineering at University of Porto. This is a network mixer that enables the fluid micro-mixing quality and intensity along the reactor [20].

The NETmix®technology concept has based on a new static mixer consisting of a regular network of spherical chambers interconnected by cylindrical channels [21]. The NETmix® reactor consists in a network interconnected chambers and channels creating zones of complete mixing and of complete segregation which are carefully designed in order to program the mixing intensity and quality, either locally as well along the reactor. This is one of the main advantages present in the NETmix® reactor when compared with other static mixers where the mixing is the difficult to control [20].

In the NETmix® reactor, mixing between different streams only occurs in the chambers. Micro-mixing depends on the mixing behaviour of the chambers and channels, where channels behave as Plug-Flow Reactors (zone of total segregation). The chambers behave as perfectly mixed Continuous Stirred Tank reactors (zones of complete micro-mixing) [20].

The NETmix® operation principle promotes strong mixing dynamics and is particularly suitable to solve many of the problems inherent to the operation of existing static mixers. It can ensure the process reproducibility for calcium phosphates nanoparticles with high purity, controlled crystallization, particle size and crystal size and morphology [20].

The goal of this reactor is produce a highly reproducible continuous process for HAP nanoparticles production with extremely high quality, based on wet chemical precipitation method [20].

Fig 10: Shows, TheNETmix® reactor applicable for HAP nanoparticles [21].

6. FOAMED BIOCERAMICS

6.1 Scaffold and porosity

A Key component in tissue engineering for bone regeneration is the scaffold that serves as a template for cell interactions and the formation of bone-extracellular matrix to provide structural support to the newly formed tissue. Scaffolds for bone regeneration should meet certain criteria to serve this function, including mechanical properties similar to those of the bone repair site, biocompatibility and biodegradability at a rate commensurate with remodelling [22].

Bone is a structure composed of HAP ($Ca_{10}(PO_4)_6(OH)_2$) crystals deposited within an organic matrix. The morphology is composed of trabecular bone which creates a porous environment with 50–90 % porosity [22].

Designed porous scaffolds should have a network of interconnected pores where more than 60 % of pores should have a size ranging from 150 to 400 µm and, at least 20 % should be smaller than 20 µm. Pores with sizes of less than 1 µm are appropriate to interact with proteins and are the main responsible for bioactivity. On the other hand, pores with sizes between 1 and 20 µm are important in cellular development. Pores of sizes between 100 and 1 000 µm play an important role in cellular and bone ingrowth, being necessary for blood flow distribution and having a predominant function in the mechanical strength of the substrate [23]. Finally, the presence of pores sizes greater than 1 000 µm will have an important role in the implant functionality and in its shape and aesthetics [23].

Scaffold properties depend primarily on the nature of the biomaterial and the fabrication process.

Porosity is defined as a percentage of void space in a solid and it is a morphological property independent of the material [24]. Pores are necessary for bone tissue formation because they allow migration and proliferation of osteoblasts and mesenchymal cells, as well as vascularization [25].

In addition, a porous surface improves mechanical interlocking between the implant biomaterial and the surrounding natural bone, providing greater mechanical stability at this critical interface. The most common techniques used to create porosity in a biomaterial are salt leaching, gas foaming, phase separation, freeze-drying and sintering depending on the material used to fabricate scaffold. The minimum pore size required to regenerate mineralized bone is generally considered to be ~100 µm [26].

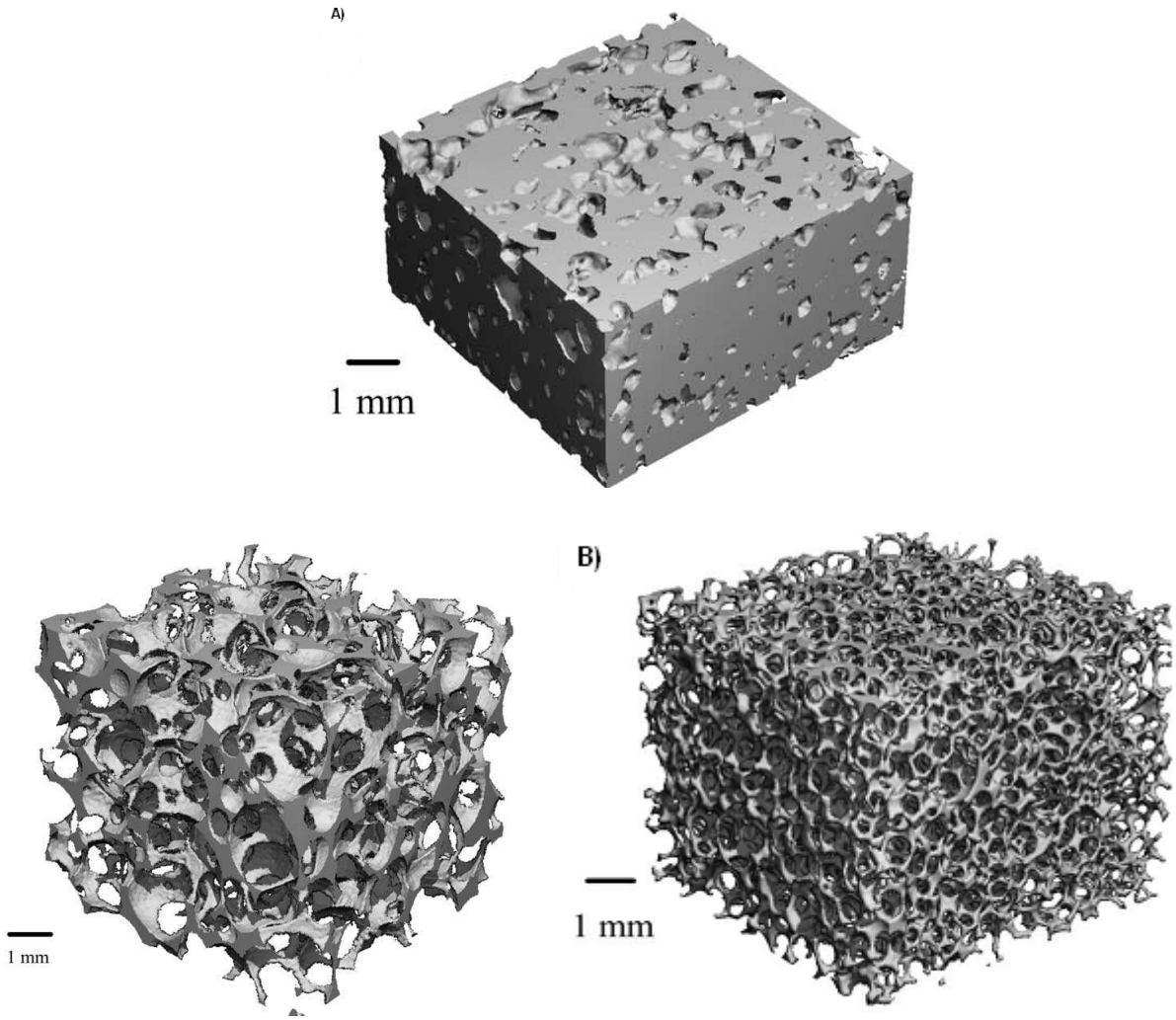

Fig. 11: Three dimensional samples by different scale porosity (A) close and (B) open porosity distribution [29].

Table 3: Requirements for ceramic-bone tissue engineering scaffold [14].

Property	**Factors**
Material property	Chemical composition (purity, crystallization) Powder processing route (commercial or lab made) raw-powder particle size and its distribution Sintering parameter (temperature and time) Mechanical properties
Porous structure property	Pore size and distribution, pore shape, porosity interconnection, micro-porosity (bulk or surface), specific surface area
Tissue interaction	Bio-compatibility, resorption rate and degradation behaviour
Geometric property	Sample size, volume and weight

6.2 Porosity material

Materials containing tailored porosity exhibit special properties and features that usually cannot be achieved by their conventional dense counter parts. Therefore, porous materials find nowadays many applications as end products and in several technological processes. Macroporous materials are used in various forms and compositions in every day life, including e.g. polymeric foams for packaging, aluminum light-weight structures in buildings and airplanes, as well as porous ceramics for water purification [27].

Contrary to metallic and polymeric porous structures, pores have traditionally avoided in ceramic components because of their inherently brittle nature. However, an increasing number of applications that require porous ceramics have appeared in the last decades, especially for environments where high temperatures, extensive wear and corrosive media are involved. Such applications include e.g. the filtration of molten metals, high-temperature thermal insulation, support for catalytic reactions, filtration of particulates from diesel engine exhaust gases, and filtration of hot corrosive gases in various industrial processes [27].

6.3 Ceramics foams

Ceramics foams are highly porous brittle materials with a closed, fully open or partially open interconnecting cellular structure. The foam structure formation, which starts from a low viscosity melt, solution, or suspension, is a complex process which generally can be divided into heterogeneous or homogeneous nucleation of gas bubbles, bubble growth and partial structure destruction by coalescence of foam cells. The final foam structure can be described as an interconnected network of irregular shaped polyhedrons [33].

Due to their low density, ceramic foam exhibit unique properties such as a high stiffness at low weight, a localized strain and fracture capability and a low thermal and electrical conductivity [33].

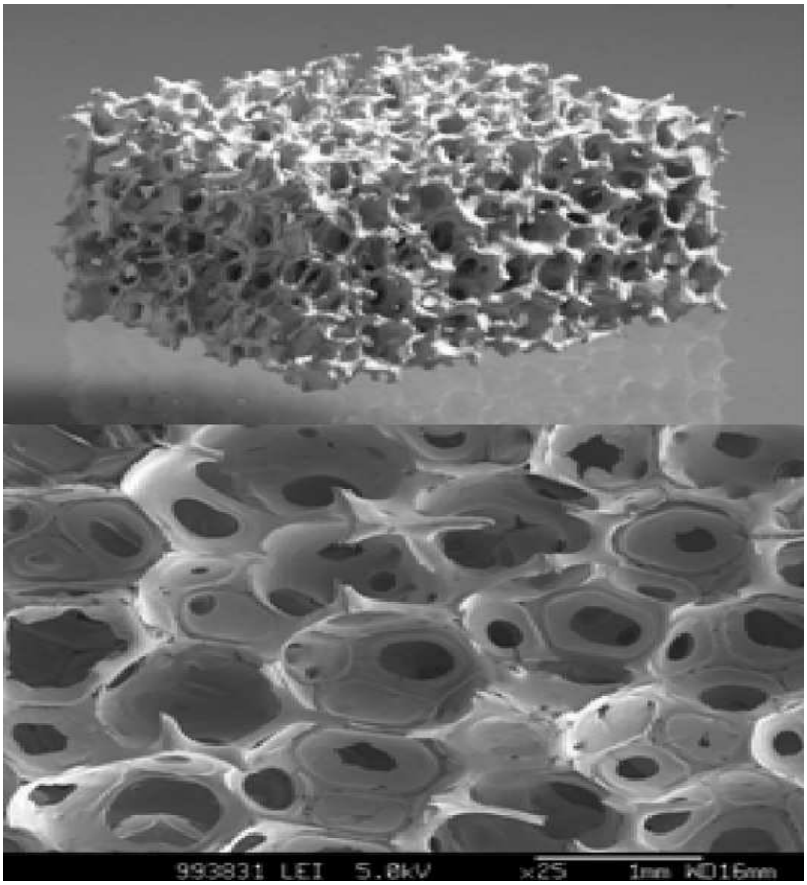

Fig. 12: Ceramic foam with his special micro-macro structure [31].

6.4 Porous HAP

HAP bioceramics apply both, in dense and porous forms. Surface area of porous bodies is much higher which guarantees good fixation and allows more cells or tissue to be carried by the implant in comparison with dense HAP. For bone ingrowth, pore size greater than 100 µm but less than 400 µm is considered to be optimum. Another important factor is the dimension of the window between the interconnected cells as the small one can prevent osteoconduction through the scaffold structure. The optimum size of the windows should be about 100 µm [28].

Porous HAP exhibits strong bonding to the bone; the pores provide a mechanical interlock leading to a firm fixation of the material. Bone tissue grows well into the pores, thus increasing strength of the HAP implant [25].

Since porous HAP is more resorbable and more osteoconductive than dense HAP. There is an increasing interest in the development of synthetic porous HAP bone replacement materials for the filling of both load-bearing and non-load bearing osseous defects [25].

6.5 Application of porous HAP

Porous HAP has applied for cell loading, drug releasing agents, chromatography analysis, and the most extensively for hard tissue scaffolds. In bone tissue engineering, it has applied as filling material for bone defects and augmentation, artificial bone graft material and prosthesis revision surgery. Various cell products are therapeutically of crucial significance including hormones, enzymes, vaccines, and nucleic acids which could improve the technology of the diagnosis and treatment of human diseases [29].

For example, chronic disease or localized surgical intervention, relying on a sustained local drug delivery needs ceramic capsule suitable to release drugs at a controlled rate. Bone drug delivery systems were also developed using porous calcium phosphate ceramics bonded with antibiotics through a biodegradable polymeric matrices. Porous HAP has extensively applied for artificial bone substitutes. The primary purpose of tissue engineering is repair, regeneration, and reconstruction of lost, damaged or degenerative tissues [29].

6.6 Preparation methods

Porous HAP can be produced by a number of methods including conversion of natural bones, ceramic foaming technique, polymeric sponge method, gel-casting of foams, starch consolidation, microwave processing, slip casting, and electrophoretic deposition technique [30].

The production techniques for cellular ceramics are generally divided into replication methods, gas bubble formation and space holder methods [30].

Great diversity of clinical reconstructive requirements for the defects of the skeleton has led to development of various methods to prepare porous ceramic implants. This is to allow design and production of porous HAP with controlled porosity and good pore interconnectivity [29].

6.6.1 Formation of porous structure – burn away during sintering

Porosity can be increased by adding fillers. Various kinds of pore making agents including paraffin, naphthalene, carbon, starch, flour, hydrogen peroxide, or synthetic polymers (e.g. polyvinyl butyral) are admixed to HAP powders or slurries. After moulding, the organics burn away from the moulding body during sintering. This approach allows direct control over the pore characteristics since their fraction, size, morphology, and distribution are controlled by type, amount and properties of the added volatile phase. Obtained porous ceramics usually have closed macro-pores with a varied pore size of 0.1–5 000 µm diameter [29].

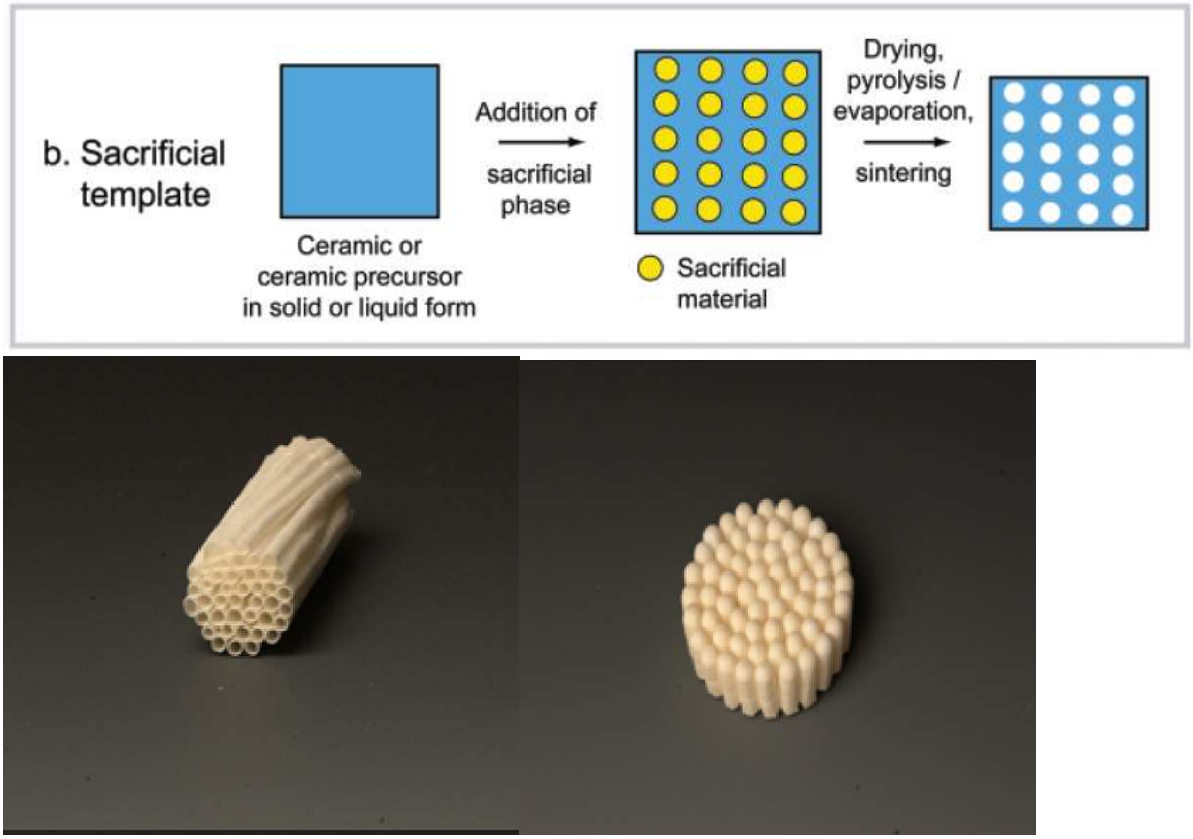

Fig. 13: Examples of the hollow beads method with sacrificial template [27, 31].

6.6.2 Holder methods

It consists of mixing salt crystals and water soluble polymers as pore creating agents with calcium phosphate powders followed by cold-isostatic pressing. Since porogens are easily water soluble they can be removed without any heat treatment. Pores are formed by the salt crystals and channels between these pores are formed by the polymeric fibres. The obtained porous HAP showed good pore interconnectivity with the pore diameters in the range of 250–400 µm [29].

6.6.3 Ceramic foaming technique

This technique involves foaming of ceramic suspensions or swelling of ceramic green bodies via gas evaporating chemical reactions from organic and inorganic sources. Some foaming agents tested were hydrogen peroxide, carbonate salt, and baking powder. They were added to the HAP slurries while stirring to let it foam, and them subjected to polymerization followed by sintering [29].

Porous HAP has obtained pore sizes of 30–600 µm [29]. The most successful method for foaming bioactive ceramics is the gel-casting method [31].

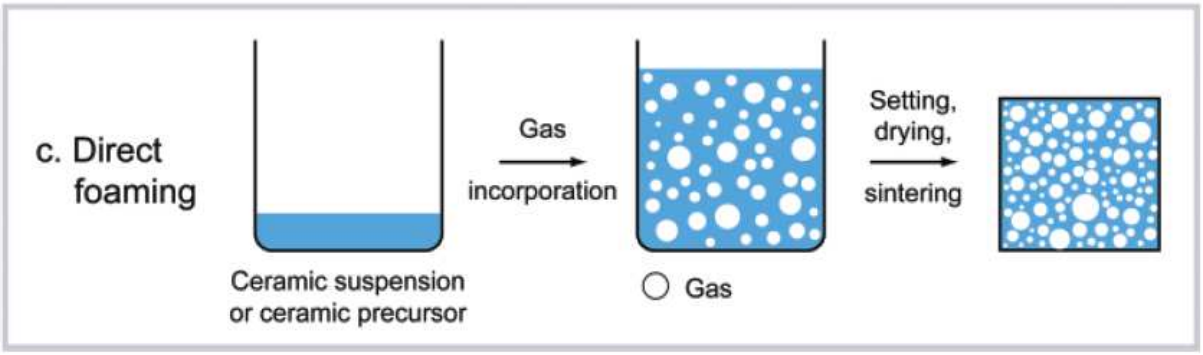

Fig. 14: Scheme of possible processing route used for the direct foaming [27].

6.6.3.1 Gel-casting method

For the gel-casting method, the powder slurry was prepared containing a foaming and gelling agent. The second step was the mechanically foaming of the suspension which was casted in mould and gelled. Hereafter, the structure was thermally treated: the drying, the calcining and the sintering [32].

Suspensions of HAP particles, water and dispersing agents and organic monomers were foamed by agitation at with the addition of surfactant under a nitrogen atmosphere. In *situ* polymerisation of the monomers was initiated and cross-linking occurred, forming a 3D polymeric network (gel), which produced strong green bodies. The polymerisation process was initiated by catalyst before casting. Porous samples were then sintered to provide mechanical strength and to burn out the organic solvents [31].

The wall surface of the device obtained is very smooth and HAP particles are aligned closely to one another and bound tightly. With average pore size 150 µm and average inter-pore connections 40 µm, this device is favourable for inter-pore cell migration or tissue ingrowth. Gel-casting of foams can be applied to produce ceramic scaffolds with high mechanical strength. The disadvantage of this technique is that it typically results in a structure of poorly interconnected pores and non-uniform pore size distribution [29].

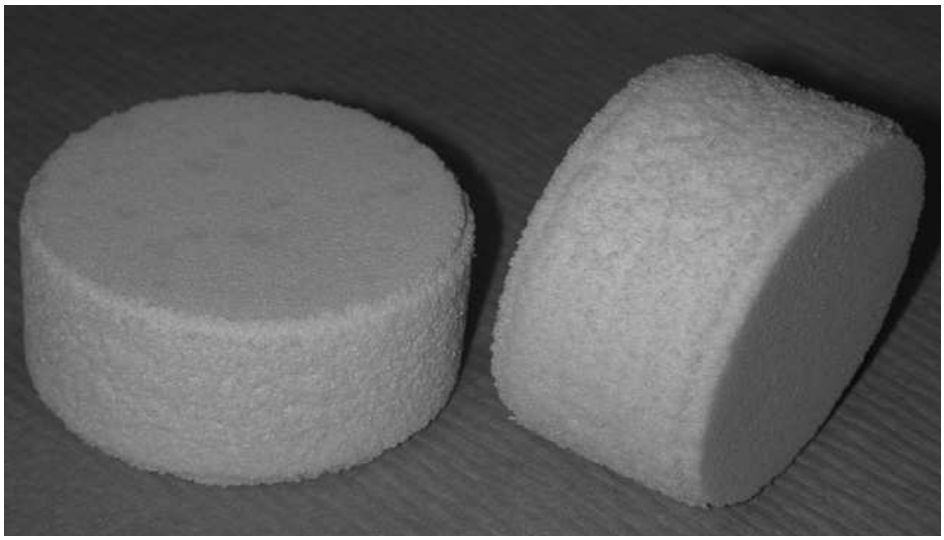

Fig. 15: Gel casted Al_2O_3 [31].

6.6.4 Polymeric sponge method

Porous ceramics obtained from reticulated polymer substrates have a number of distinct properties such as controllable pore size and complex ceramic shapes suitable for different applications. The polymeric sponge method, as this method named is performed by impregnating porous polymeric substrates (sponges) with HAP slurry. Porous HAP prepared via the polymeric sponge method has shown well-interconnected pores but poor mechanical strength for load bearing applications. It was shown that the polymeric sponge method results in a proper pore size distribution, as osteoconduction requires. This is characterized by the existence of micro/meso/macro-pores with adequate degree of interconnection [29].

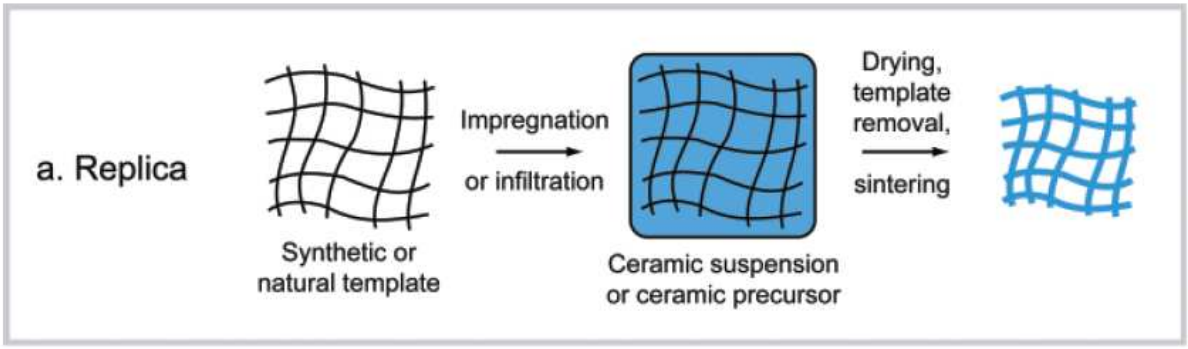

Fig. 16: Scheme of possible processing route used for replica (polymeric sponge method) [27].

6.7 Mechanical behaviour

However, due to their high porosity these ceramics have comparatively low mechanical stability. Depending on the ceramic material the compressive strength can get as low as 0.16 MPa for HAP at a porosity of 87 %. Similarly low values were reported for other ceramic materials such as Al_2O_3 (0.3 MPa, porosity 87 %). As such weak ceramics need to be handled with great care, increasing their strength is of interest. One way for improving their strength is to apply additional ceramic coatings. This can result in an unfavorable reduction of the intentionally high porosity. [33].

Mechanical properties of porous scaffolds also depend on the compositional design of the scaffold. To avoid the brittleness of porous ceramics, many porous biodegradable polymer (such as poly(caprolactone)) to ceramic composite systems have developed [34].

Another way of using the advantages and minimizing the problems of porous bioactive/biodegradable ceramic scaffolds could be the use of a polymer coating. It has found that micro-coating the internal surfaces of porous HAP with dilactic-polyactic acid (DL-PLA) improved significantly its compressive properties [34].

6.7.1 Porosity-strength behaviour

Generally, a number of expressions can be used to describe the porosity-strength behaviour of porous ceramics. One of the simplest methods was proposed by Rice based on the minimum solid area approach and the resulting porosity-strenght dependence can be approximated closely by and exponential function [35]:

$$\sigma_0 = \sigma \cdot e^{-bp}, \qquad [3.1]$$

σ_0 is zero porosity strength, σ is the strength at pore volume fraction p, and the constant b is related directly to the pore characteristics [35].

7. EXPERIMENTAL PART

The practical part was aimed at preparation of HAP by 3 methods (precipitation, sol-gel in water and ethanol). The microstructure of each sample has evaluated by SEM methods and comparing of particle size distribution.

Processing of porous HAP scaffold was prepared by 2 methods: Polymeric sponge method and direct foaming method by polymeric expancel and glass bubbles. Each of them was analyzed by SEM and Mercury Intrusion Porosimetry (MIP).

7.1 Synthesis of HAP

HAP was prepared by precipitation and sol-gel method. The molecular weight of HAP (M=502.31 g/mol) is used for determination of molecular precursors such as (Calcium nitrate and ammonium hydrogen phosphate).

7.1.1 Sol-gel methods

This is a method at low temperature followed by special characterization of pure, stable, stoichiometric synthesized HAP crystals. The tetra hydrate of calcium nitrate with formula ($Ca(NO_3)_2 \cdot 4H_2O$) for calcium cation and ammonium hydrogen phosphate ($(NH_4)_2HPO_4$) for phosphate anion were selected as the main precursors.

The chemical equation can be represented as:

$$6(NH_4)_2HPO_4 + 10Ca(NO_3) \cdot 4H_2O + 8NH_4OH \rightarrow Ca_{10}(PO_4)_6OH_2 + 20NH_4NO_3 + 20H_2O$$

$m_3 = 100.0$ g

$M_3 = 502.31$ g/mol

$M_2 = 236.15$ g/mol

$M_1 = 132.06$ g/mol

$m_2 = ?$ g

$m_1 = ?$ g

$$\frac{n_2}{n_3} = \frac{5}{1} \Rightarrow n_2 = 5n_3 \Rightarrow \frac{m_2}{M_2} = 5 \cdot \frac{m_3}{M_3} \Rightarrow m_2 = \frac{5 \cdot m_3 \cdot M_2}{M_3} = \frac{5 \cdot 100{,}0 \cdot 236{,}15}{502{,}31} = \underline{\underline{235{,}06\ g}}$$

$$\frac{n_1}{n_3} = \frac{3}{1} \Rightarrow n_1 = 3n_3 \Rightarrow \frac{m_1}{M_1} = 3 \cdot \frac{m_3}{M_3} \Rightarrow m_1 = \frac{3 \cdot m_3 \cdot M_1}{M_3} = \frac{3 \cdot 100{,}0 \cdot 132{,}06}{502{,}31} = \underline{\underline{78{,}87\ g}}$$

The Ca/P ratio for stoichiometric HAP is 1.67. It is necessary for biological response and producing a pure HAP without minor fraction.

Slight imbalances in the ratio of Ca/P can lead to the appearance of extraneous phases. If the Ca/P ratio is lower than 1.67, then alpha or beta tricalcium phosphate may be present after processing. If the Ca/P is higher than 1.67, calcium oxide (CaO) may be present along with the HAP phase [7].

For the sol-gel chemistry routes, the water and ethanol were used as a solvent. During preparing solution the $Ca(NO_3)_2 \cdot 4H_2O$ was added to $(NH_4)_2HPO_4$ solution (in vigorous stirring). The pH was maintained and keeping about 9–10. The temperature was heating until 65 °C (for water) and 80 °C (for ethanol) with evaporation and continuous stirring during several hours. After transforming from sol to gel the viscosity was increasing rapidly. The white color gel was several time decadate to neutral pH only in water solution.

After allowing the product of HAP to cool, it was oven dried at 100 °C over night. The dry samples have introduced for sintering to furnace.

7.1.2 Synthesis of HAP by precipitation method

Precipitation is the formation of a solid in a solution or inside another solid during a chemical reaction or by diffusion in a solid. When the reaction occurs in a liquid, the solid formed is called the precipitate [37].

The solubility equilibrium was generally established:

$$S_{A_nB_n} = [A]^n \cdot [B]^n \qquad [4.1]$$

Hydroxyapatite was prepared by water solution-precipitation method using $Ca(NO_3)_2 \cdot 4H_2O$ and $(NH_4)_2HPO_4$. A suspension was prepared at laboratory temperature. The pH of suspension was keeping about 9–10. After precipitate the water slurry was several times washing to neutral pH, filtrate, drying and finally sintering. The chemical equation is similar as the sol-gel method with the identical stochiometric balances of precursors.

7.2 HAP foamed preparing

Porous hydroxyapatite was prepared by two methods: polymeric sponge method and direct foaming by polymeric expancel and glass bubbles. The process outline of each method has described and investigated in the following section. Every part has characterized by the porosity measurement and Mercury Intrusion Porosimetry (MIP). Finally, it has compared the porosity affection by the sol-gel method and precipitaton as well as the comparing of polymeric sponge method versus the direct foaming method.

7.2.1 HAP scaffold by polymeric sponge method

The polymeric sponge method is performed by the synthetic template (concretely by the polyurethane sponge with regular diameter) and HAP slurry. The HAP slurry is applied by the sol-gel as well as precipitation methods. The porous polymeric substrates (sponge) are impregnated in the HAP slurry. Sponge pieces (3×3×2) were pressed in HAP slurry during several hours for quality impregnation. After soaking, the soaked sponge was oven dried at 100 °C over night. The dried sponge was calcined by three steps and after sintered. The first temperature was established to 300 °C, the second one to 600 °C and that last one to 1 000 °C. The samples were kept at these temperatures for one hour for binder burnt out.

Porosity, pore size distribution, microstructure and surface porosity area of the sintered porous scaffold were characterized.

7.2.2 HAP scaffold by foaming agent

Typical foaming technique as call them direct foaming were realize. This may be use for ceramic suspension or precursor. It has prepared the HAP slurry by sol-gel (ethanol) and precipitation method way. This slurry has poured to corundum cylinder cups in dimension (3×3×2). The poured samples were filled up by polymeric expancel (2 wt.%) and glass bubbles to HAP slurry (100 wt.%). After mixture, the samples were oven dried at 100 °C over night. The dried samples were sintered to 1 200 °C for 1 hour at a heating reat of 5 °C per minute. The polymeric expancel was marked as 951 DUX 120. The glass bubbles was marked as 3M™ Scotchlite™ Glass Bubbles.

7.2.2.1 Glass Bubbles

3M™ Scotchlite™ Glass Bubbles are engineered hollow glass microspheres that are alternatives to conventional fillers and additives such as silicas, calcium carbonate, talc, clay, *etc*., for many demanding applications. These low density particles are used in a wide range of industries to reduce part weight, lower costs and enhance product properties [50].
The unique spherical shape of Scotchlite glass bubbles offers a number of important benefits, including: higher filler loading, lower viscosity/improved flow and reduced shrinkage and warpage [50].

- **3M™ Scotchlite™ Glass Bubbles**

These bubbles are specially formulated for a high strength-to-weight ratio. They also produce stable voids, which results in low thermal conductivity and a low dielectric constant. Scotchlite glass bubbles are available in a variety of sizes in our case the diameter is in range 200–400 µm [50].

7.2.2.2 Polymeric expancel

Expancel microspheres are small spherical thermoplastic particles. The microspheres consist of a polymer shell encapsulating a gas. The average diameter of these hollow spheres range from 6 to 45 µm and have a true density of 1 000 to 1 300 kg/mł (8.3–10.8 lbs/US Gallon). Fully expanded the volume of the microspheres has increased more than 40 times (with the diameter changing, for example, from 10 to 40 µm), resulting in a true density below 30 kg/mł (0.25 lbs/US Gallon). Typical expansion temperatures range from 80 to 190 °C (176–374 °F). When heating the microspheres the pressure of the gas inside the shell increases and the thermoplastic shell softens, resulting in a dramatic increase of the volume of the microspheres. Cooling the microspheres results in the shell stiffening again and light expanded microspheres are ready for use [38].

- **951 DUX 120**

The particle size is 28–38 µm. The thermomechanical analysis (starting temperature T_{start}=133–134 °C, T_{max}=190–205 °C) [38].

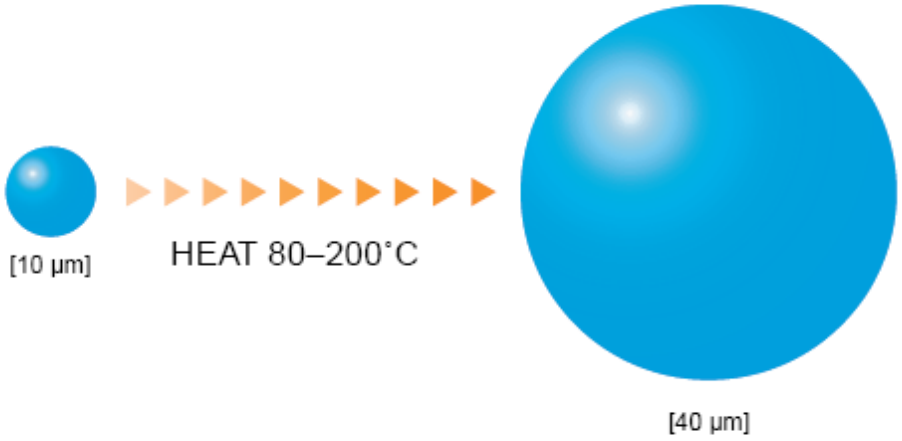

Fig. 17: Progressive particle expanding during heating [38].

7.3 HAP sintering

Sintering of ceramic materials is the method involving consolidation of ceramic powder particles by heating the "green" compact part to a high temperature below the melting point, when the material of the separate particles difuse to the neighbouring powder particles. Sintering of pure oxide ceramics require relatively long time and high temperature because the diffusion proceeds in solid state [39].

Decrease of the porosity, caused by the sintering process, is determined by the level of the initial porosity of the "green" compact, sintering temperature and time [39].

The grain size of sol-gel prepared powder products was measured by using the Scherer´s equation [40]:

$$t = 0{,}89\lambda / B \cdot \cos\theta\,, \qquad [5.1]$$

where t is grain size, λ is wavelength of the X-ray tube, B is width of peak in the middle of its height and θ is Bragg´s angle [40].

By the increasing the temperature and time of sintering treatment process, the particle size of powder will be increased [40].

The nano-scale of HAP particles is the main assumption for accepting by the host tissue.

7.4 Bioactive test of HAP

Bioactivity test was done by taking of SBF (Simulated body fluid). SBF prepared in accord with the chemical analysis of human body fluid, with ion concentrations nearly equal to those of the inorganic constituents of human blood plasma [41].

Table 4: Typical chemical parts in SBF (number of compound (g)/ in 1 litre destilled water) [42].

Composition of chemical compound in SBF	quantity (g)
Sodium chloride (NaCl)	8.218 7
Potassium chloride (KCl)	0.226 0
Di hydrate calcium chloride ($CaCl_2 \cdot 2H_2O$)	0.386 0
Sodium hydrogen carbonate (Na_2HCO_3)	0.350 8
Tri hydrate potasium hydrogen phosphate ($K_2HPO_4 \cdot 3H_2O$)	0.333 7
Deca hydrate sodium sulfate ($Na_2SO_4 \cdot 10H_2O$)	0.169 7
Hexa hydrate magnesium chloride ($MgCl_2 \cdot 6H_2O$)	0.336 6

When porous HAP is treated in SBF solution, at first, on soaking in SBF, the surface structural change occurs in HAP resulting in the formation of a Ca-rich ACP on their surfaces. In view of change in Ca/P ratio, the formation of Ca-rich ACP is a consequence of interaction of the HAP surface specifically with the calcium ions in the SBF. The second surface structural change is the formation of Ca-poor ACP, for which the HAP appear to use the Ca-rich ACP on their surfaces to interact with the phosphate ion in the fluid. The third surface structural change is the formation of apatite. The Ca-poor ACP on the HAP appears to gradually crystallize into bone like apatite, through which the HAP appear to stabilize their surfaces in SBF [43].

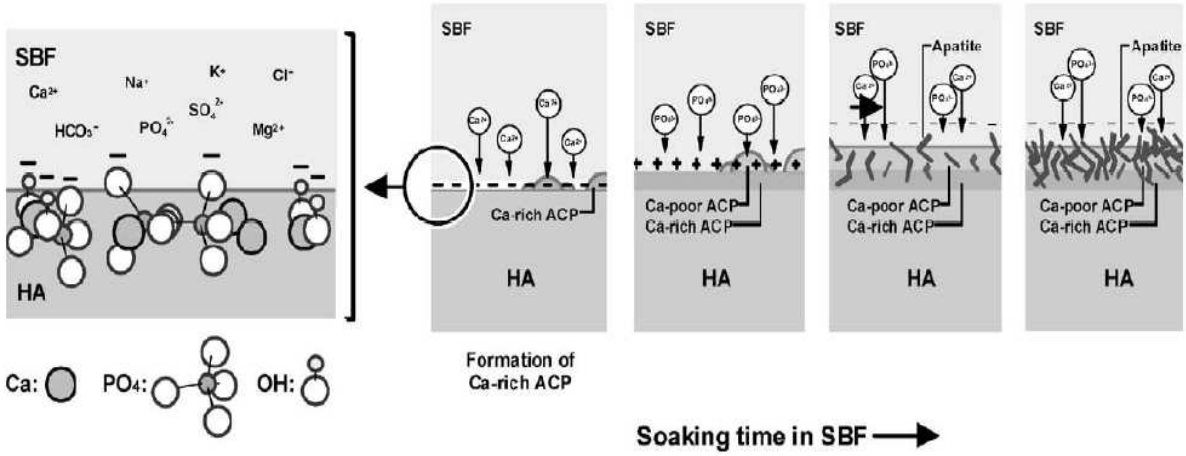

Fig. 18: Schematic presentations of the origin of negative charge on the HAP surface and the process of bone like apatite formation in SBF [43].

7.5 Characterizations

7.5.1 Phase analysis (XRD)

X-ray diffraction is now a common technique for the study of crystal structures and atomic spacing. X-ray diffraction is based on constructive interference of monochromatic X-rays and a crystalline sample. These X-rays are generated by a cathode ray tube, filtered to produce monochromatic radiation, collimated to concentrate, and directed toward the sample. The interaction of the incident rays with the sample produces constructive interference (and a diffracted ray) when conditions satisfy Bragg's Law ($n\lambda=2d \sin\theta$). This law relates the wavelength of electromagnetic radiation to the diffraction angle and the lattice spacing in a crystalline sample. These diffracted X-rays are then detected, processed and counted. By scanning the sample through a range of 2θ angles, all possible diffraction directions of the lattice should be attained due to the random orientation of the powdered material. Conversion of the diffraction peaks to d-spacings allows identification of the mineral because each mineral has a set of unique d-spacings. Typically, this is achieved by comparison of d-spacings with standard reference patterns [44].

7.5.2 Infrared spectroscopy (IR spectroscopy)

This is the spectroscopy that deals with the infrared region of the electromagnetic spectrum, that is light with a longer wavelength and lower frequency than visible light. It covers a range of techniques, mostly based on absorption spectroscopy. A common laboratory instrument that uses this technique is a FTIR [45].

The infrared portion of the electromagnetic spectrum is usually divided into three regions; the near-, mid- and far-infrared, named for their relation to the visible spectrum. The higher energy near-IR, approximately 14 000–4 000 cm^{-1} (0.8–2.5 μm wavelength) can excite overtone or harmonic vibrations. The mid-infrared, approximately 4 000–400 cm^{-1} (2.5–25 μm) may be used to study the fundamental vibrations and associated rotational-vibrational structure. The far-infrared, approximately 400–10 cm^{-1} (25–1 000 μm), lying adjacent to the microwave region, has low energy and may be used for rotational spectroscopy [45].

7.5.3 Scanning electron microscope (SEM)

A scanning electron microscope (SEM) is a type of electron microscope that images a sample by scanning it with a beam of electrons in a raster scan pattern. The electrons interact with the atoms that make up the sample producing signals that contain information about the sample's surface topography, composition, and other properties such as electrical conductivity [46].

The electron beam, which typically has an energy ranging from 0.2 keV to 40 keV, is focused by one or two condenser lenses to a spot about 0.4 nm to 5 nm in diameter. The beam passes through pairs of scanning coils or pairs of deflector plates in the electron column, typically in the final lens, which deflect the beam in the *x* and *y* axes so that it scans in a raster fashion over a rectangular area of the sample surface. When the primary electron beam interacts with the sample, the electrons lose energy by repeated random scattering and absorption within a tear drop-shaped volume of the specimen known as the interaction volume, which extends from less than 100 nm to around 5 µm into the surface [46].

7.5.4 Mercury Intrusion Porosimetry

Mercury intrusion porosimetry is an analytical technique that can determine many of the sought-after physical characteristics of raw materials and green ware [47].

This is a method used to measure both porosity and pore sizes. The scaffolds are placed in a penetrometer and infused with mercury under increasing pressure. As the pressure (P) increases, the radius of pores (r) that can be filled decreases according to the Washburn equation [14]:

$$D = -4\gamma \cos\theta / P\,, \qquad [6.1]$$

where P is the applied pressure, γ the surface tension of the mercury, θ the contact angle between the mercury and solid surface, and D the smallest diameter of an opening into which mercury will penetrate at pressure P [47].

8. RESULTS AND DISCUSSION

Table 5: Results of preparation HAP by different methods.

Method	Temperature [°C]	Dominant phase	Chemical structure	Content (%)	Minority phase	Chemical structure	Content (%)
Sol – gel (water)	1000	HAP	hexagonal	73	β-TCP α-TCP	Rhombohedral Monoclinic	9 18
precipitation (water)	1000	HAP	hexagonal	52	β-TCP	Rhombohedral	48
Sol – gel (ethanol)	1000	HAP	hexagonal	79	β-TCP	Rhombohedral	21

Sol-gel and precipitation methods were used to prepare HAP. The sintering temperature was established at 1 000 °C. It shoud obtain HAP as main phase supplemented by a minor phase of TCP (specially β form).

The semi-quantitative and semi-qualitative results of the main phases are reported in Table 5.

An ideal composition called biphasic calcium phosphate (BCP) ceramics have developed consisting of HAP and ß-TCP in the wt.% ratio of approximately 70:30 and is performing better in *vivo* in the long term application

For this purpose we can express the ideal preparing sample by sol-gel method (in ethanol) or more less by sol-gel method (in water).

TCP can exist under three polymorphs, such as [48]:

β-TCP stable below 1 120 °C with a density equal to 3.07 g/cc

α-TCP stable between 1 120 and 1470 °C with a density equal to 2.86 g/cc

α´-TCP stable above 1 470 °C

Generally, β-TCP densification is difficult because the low temperature of $\beta \rightarrow \alpha$ phase transformation does not permit the sintering to high temperature. Indeed, this phase transformation hinders the TCP densification and on the other hand, induces micro-cracking of that sample due to the material expansion generated by density mismatch between β and α phases [48].

HAP and ß-TCP not only differ in composition but also in their rate of degradation. ß-TCP has shown to biodegrade or bioresorb more readily than HAP, but in an unpredictable way, so it may not provide a scaffold for new bone to grow [49].

ß-TCP is degraded 10–20 times faster than HAP. It generally results in superior remodelling than HAP during the final stage of bone formation. It is note worthy that ß-TCP is resorbed by osteoclast cells, whereas, the much slower resorption of HAP is effected mainly by foreign-body giant cells. The giant cells have a limit as to the amount of HAP they will resorb [49].

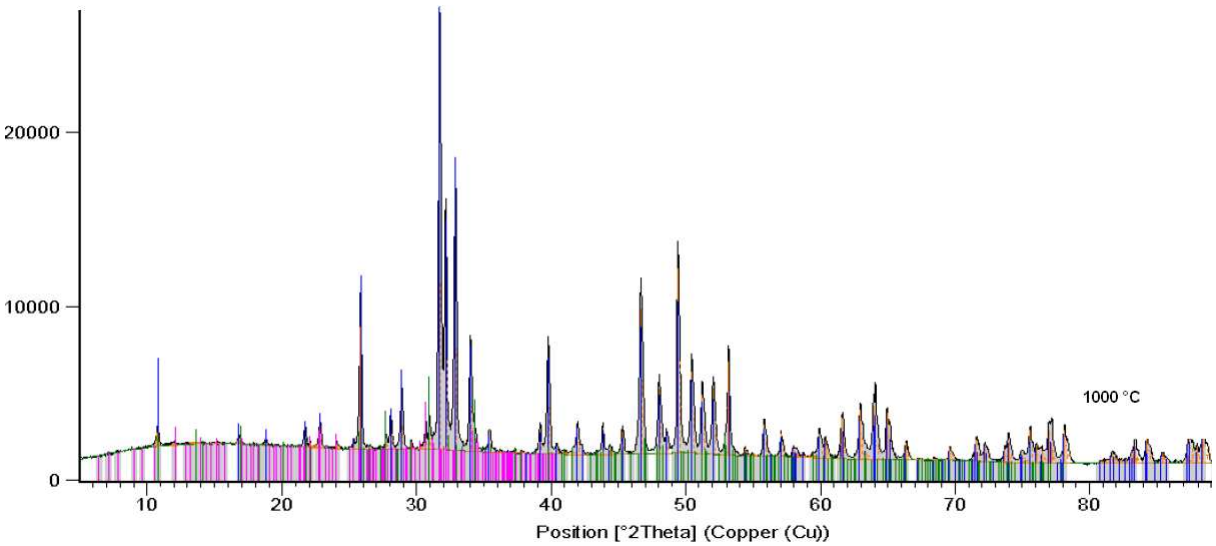

Fig. 19: X-ray diffraction (XRD) patterns of the samples: a) method indicates the phases of HAP in sol-gel (water) after sintering at 1 000 °C.

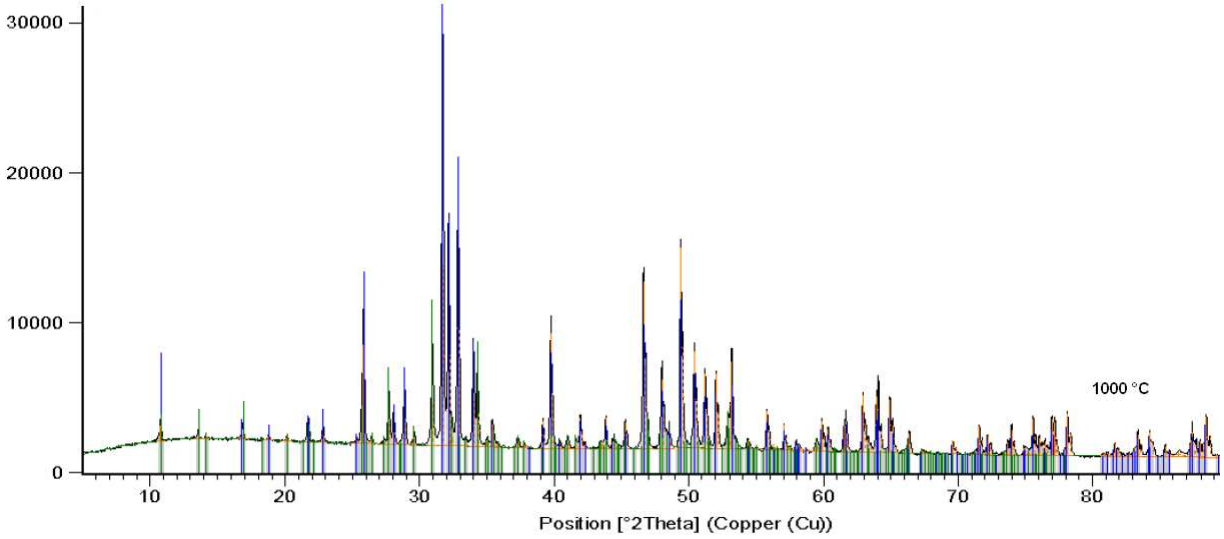

Fig. 20: X-ray diffraction (XRD) patterns of the samples: b) method indicates the phases of HAP in sol-gel (ethanol) after sintering at 1 000 °C.

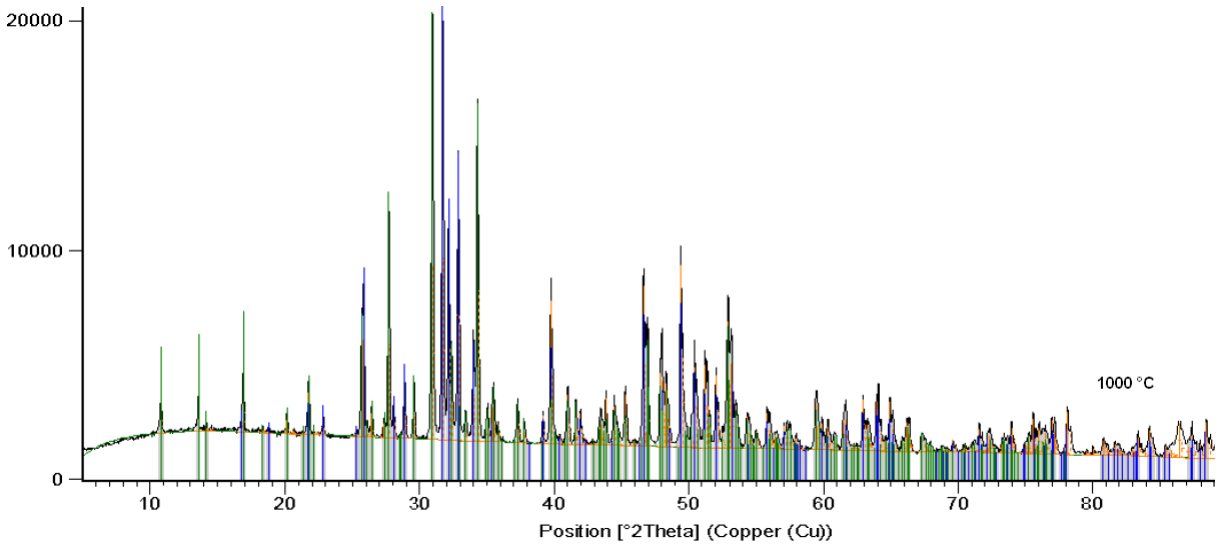

Fig. 21: X-ray diffraction (XRD) patterns of the samples: c) method indicates the phases in precipitation after sintering at 1 000 °C.

The IR spectrum is divided into 3 regions in mid infrared range at 4 000–500 cm^{-1} frequency. The IR spectrum of raw HAP shows (Fig. 23) the bands corresponding to PO_4^{3-} group at 1 090 cm^{-1} and 1 040 cm^{-1}, other area is located near 600 cm^{-1} characterized by (P-O group) for generally phosphorous function. The last one is assigned in the bands at 3 500 cm^{-1} to (OH group) for HAP. The position of the carbonate bands indicate that the CO_3^{2-} groups are observed at 1 470–1 440 cm^{-1}.

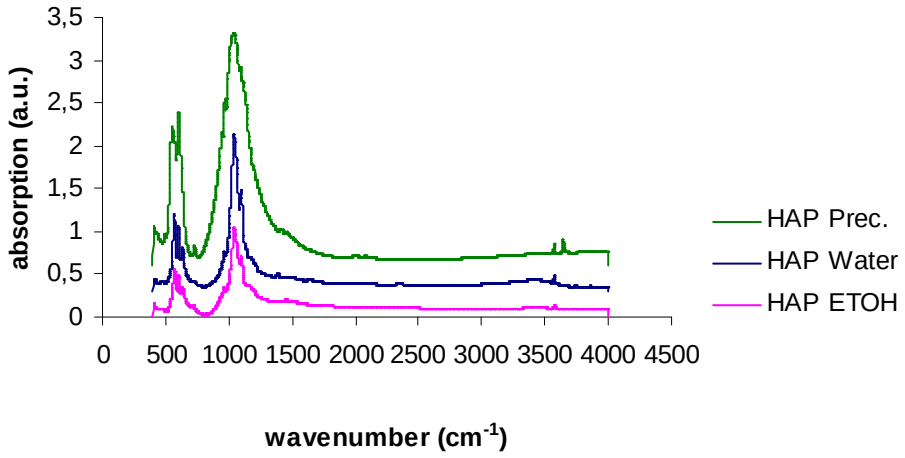

Fig. 22: FTIR spectra of HAP powder prepared by various methods and calcined at 1 000 °C.

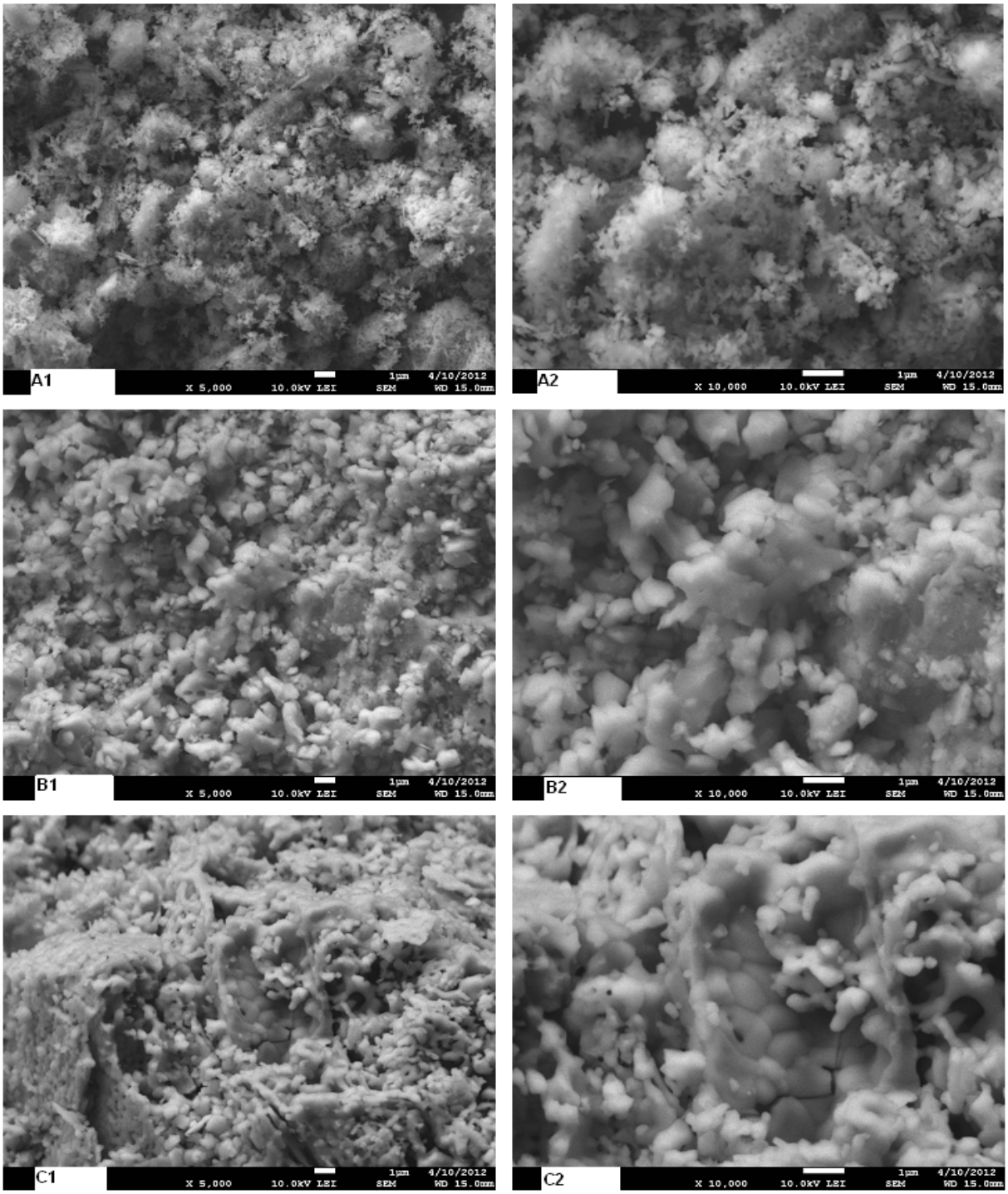

Fig. 23: SEM image showing the HAP particles produced in three methods sintered at 1 000 °C: A) sol-gel in water, B) sol-gel in ethanol, C) precipitation in water. Bars: 1 µm, magnified: 5 000 × and 10 000×.

As shown in the SEM images (Fig. 23), it can be seen the particle distribution in various methods.

The sol-gel in water and ethanol produce nano-size particles as compared with precipitation method. The nano-scale particles support ossification process and bioactivity for host tissue replacement.

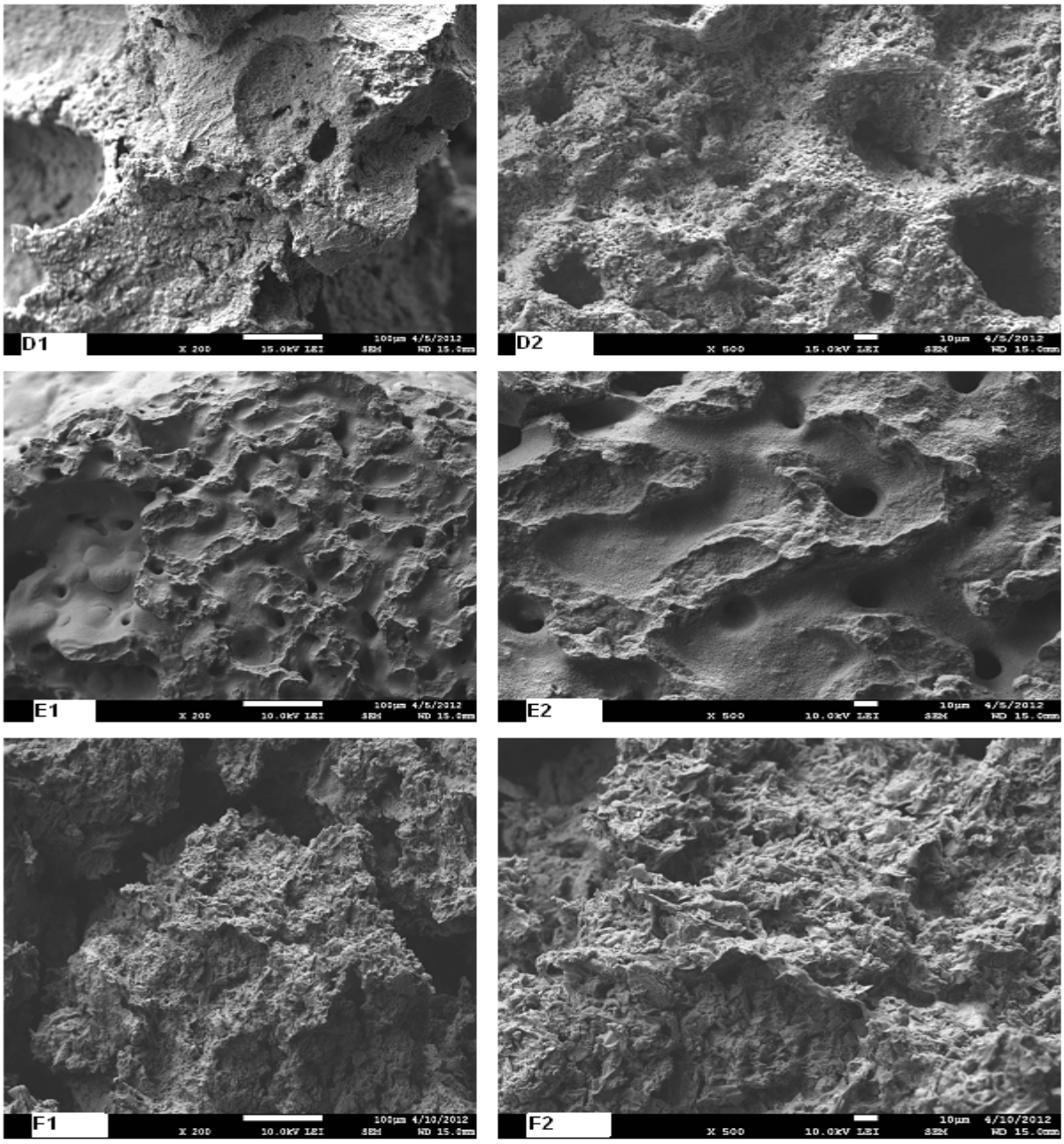

Fig. 24: SEM micrographs of the sponge polymeric scaffolds prepared from different HAP slurries: D) sol-gel in water, E) sol-gel in ethanol, F) precipitation; D1, E1, F1 Bars: 100 µm, magnified 200×, D2, E2, F2 Bars: 10 µm, magnified 500×.

SEM micrographs of different polymeric sponge scaffolds prepared from different slurries and sintered at 1 000 °C are presented in Figure 24 and Figure 25 in higher resolution. The pore structure observed at surface is variety. Polymeric sponge scaffold from HAP prepared by sol-gel method in water presents large pores isolated. By observing pore walls (Figure 25, D4), one can remark the presence of fine particles with extraparticle pores. The structure of pore walls is not compact. The macro pores with dimension in the range 60–100 µm (D1, D2) meso pores in range 10–20 µm (E1, E2) were obtained by using polurethane foam, as shown in Fig. 24, 25.

Contrary to Fig. 24 D1-D2 and Fig. 25 D3-D4, SEM of scaffold from HAP synthesis via sol-gel method in ethanol presents closed and interconnected pores at surface. Some pores have hole aspect. Detail in microstructure of pore wall show very fine and dense particles forming a compact structure. The extraparticle pore seems to be absent. It was observed that pore distribution of scaffold from HAP synthesised by sol-gel method is regular (shows in E1, E2 and E3, E4 images).

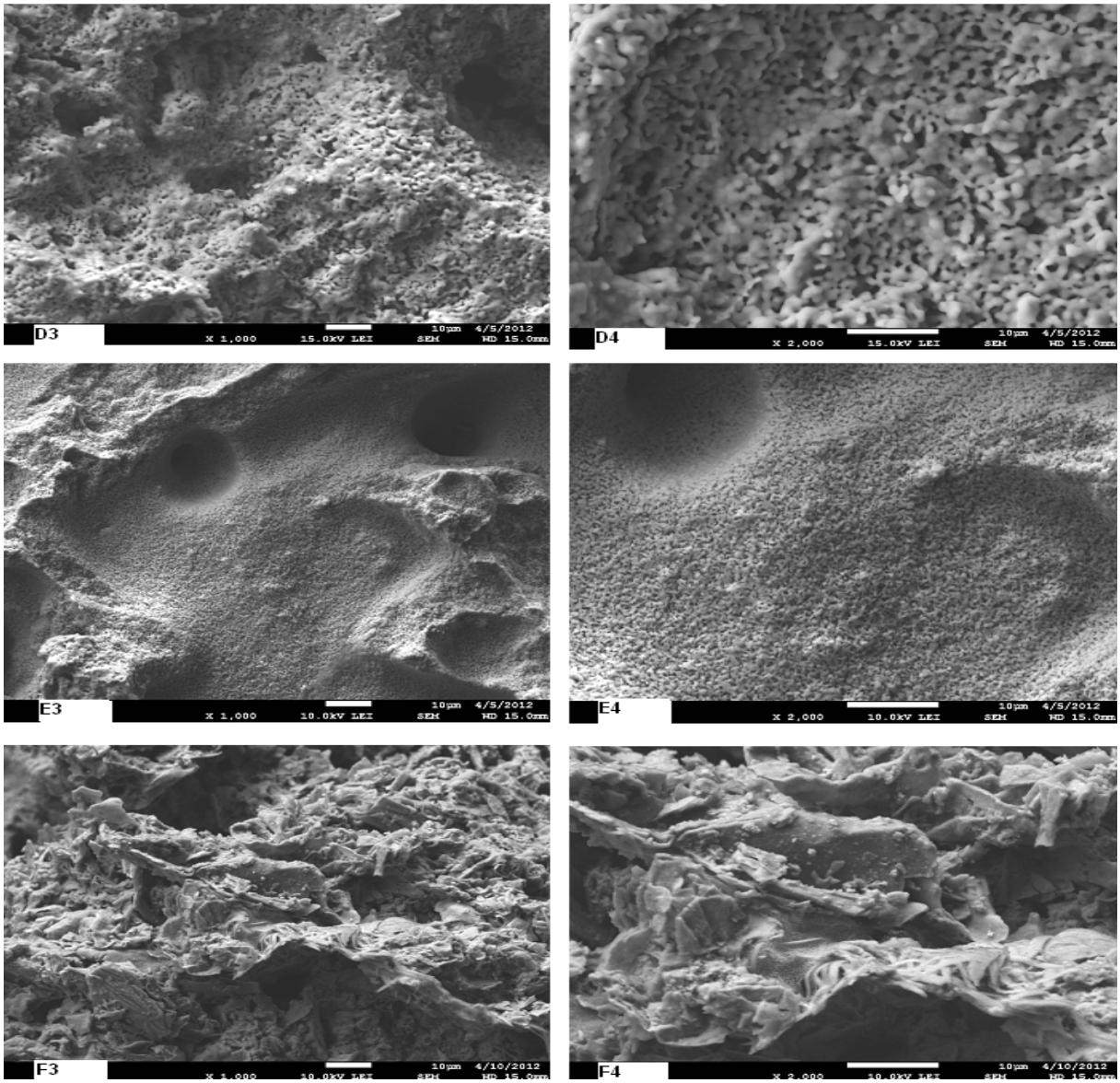

Fig. 25: SEM micrographs of the sponge polymeric scaffolds at different HAP slurries: D) sol-gel in water, E) sol-gel in ethanol, F) precipitation; D3, E3, F3 Bars: 10 µm, magnified 1 000×, D4, E4, F4 Bars: 10 µm, magnified 2 000×.

Scaffolds made from HAP synthesis by precipitation method presents no visible pore at surface. As the particles were coarse, it seems that they were immerged in mass. Referring to these findings, one can state that the precipitation by polymeric sponge method is not appropriate method to create pore structure, as it can be seen from F1-F4.

The pore structure with low pore interconnectivity is of relatively low interest for medical purposes, in particular for tissue engineering scaffold applications.

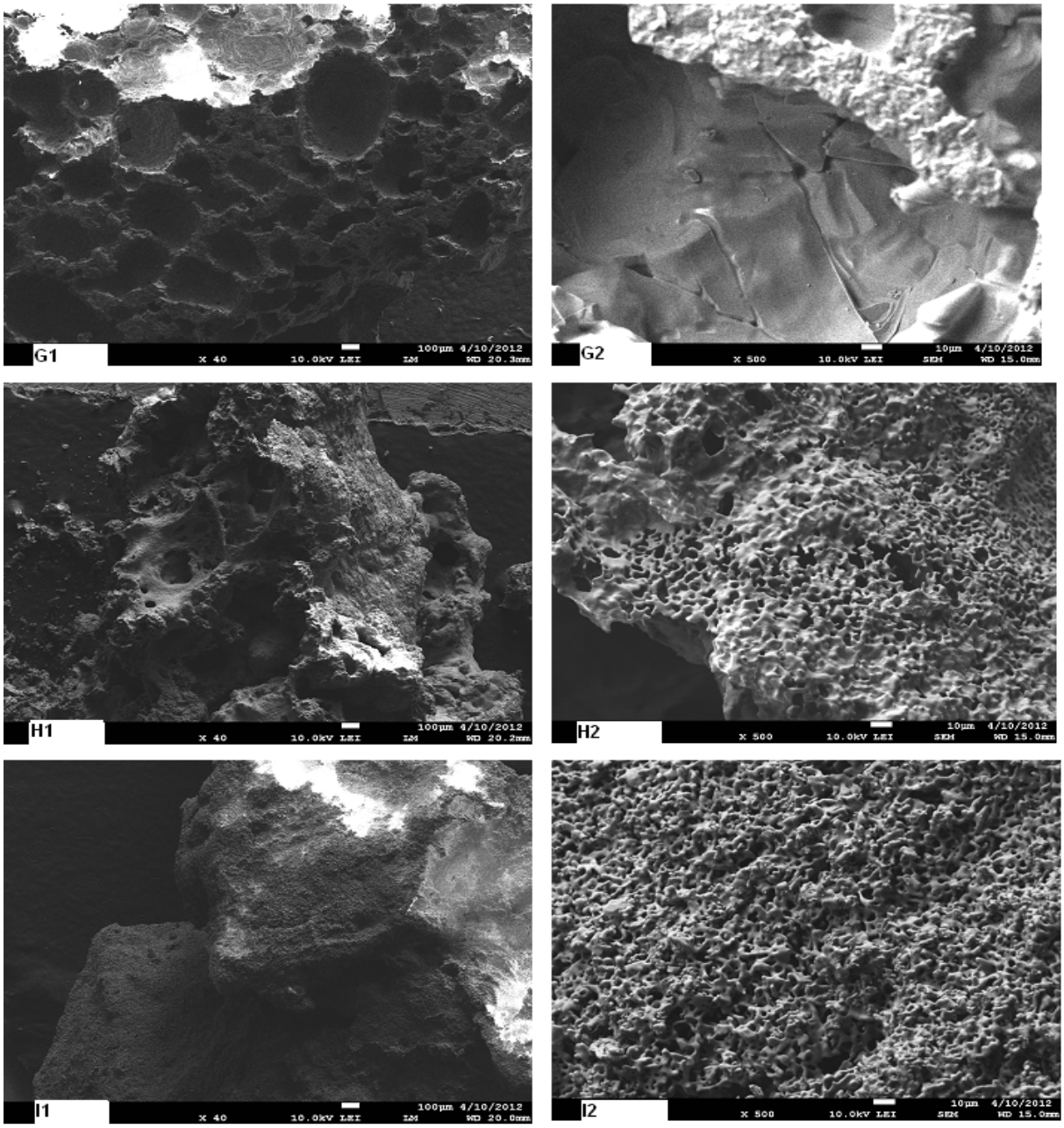

Fig. 26: SEM micrograph showing the morphology of direct foaming method derived-porous HAP with the porosity gradient. G) sol-gel in ethanol by glass bubbles H) sol-gel in ethanol by DUX expancel, I) precipitation by DUX expancel; G1, H1, I1 Bars: 100 µm, magnified: 40×; G2, H2, I2 Bars: 10 µm, magnified: 500×.

The SEM structure of the sintered foamed ceramics by direct foaming is presented in Fig. 26, 27.

The obtained porous scaffold was typically composed of approximately spherical cells interconnected by circular windows, as shown us Fig. 26 G1. The macro pores with dimension in the range 400–600 µm (G1) were obtained by using glass bubbles, as shown in Fig. 26.

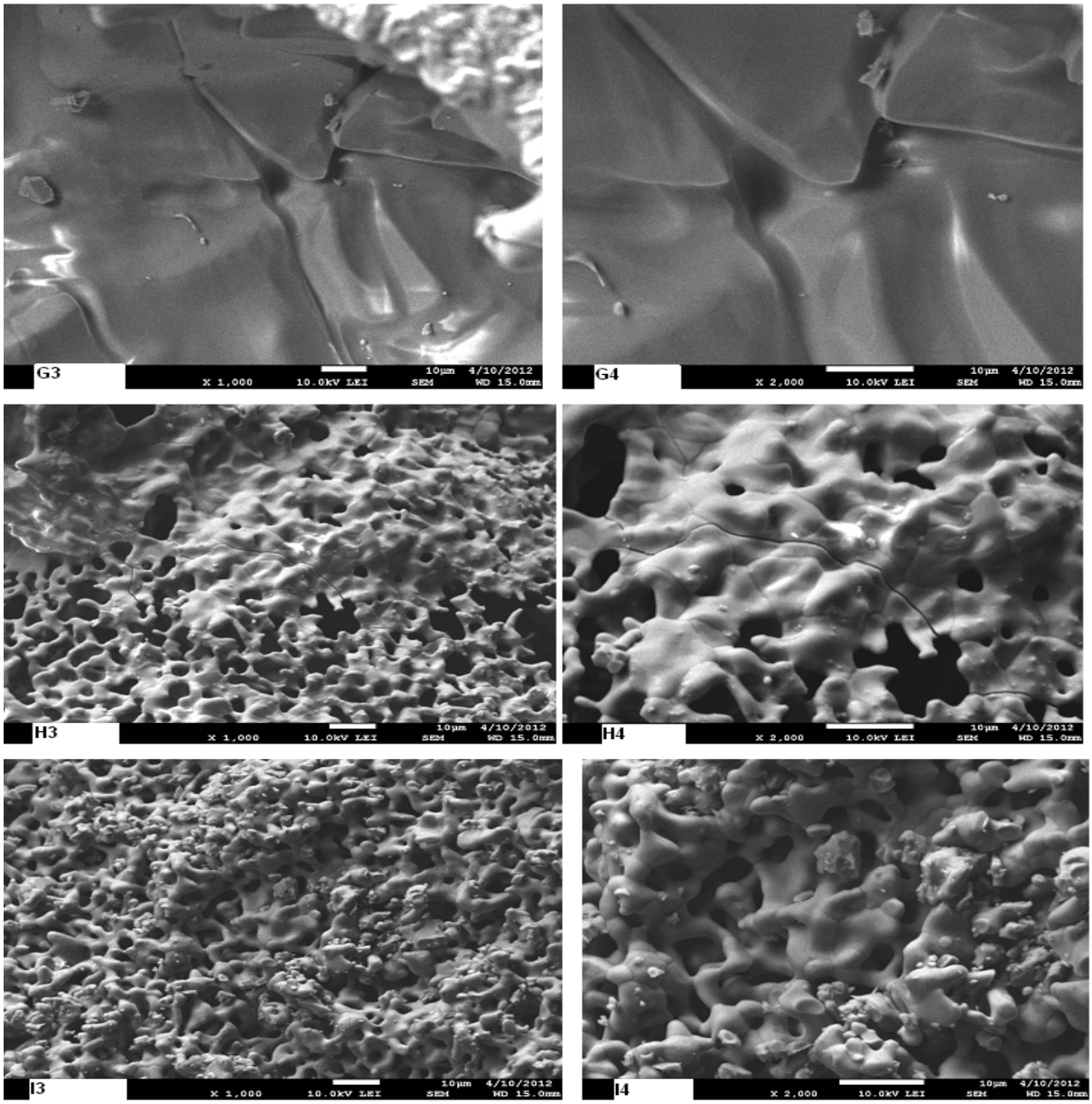

Fig. 27: SEM micrograph showing the morphology of direct foaming method derived-porous HAP with the porosity gradient. G) sol-gel in ethanol by glass bubbles, H) sol-gel in ethanol by DUX expancel I) precipitation by DUX expancel; G3, H3, I3 Bars: 10 µm, magnified: 1 000×; G4, H4, I4 Bars: 10 µm, magnified: 2 000×.

However, in samples G1-G4 a higher sintering degree was observed as well as a higher density and pore´s size (especially macro pores). However, the using of polymeric expancel has improved the microstructure (especially in I3-I4 and H3-H4) representing the precipitation in water and the sol-gel in ethanol, respectively.

The grain microstructure of the spherical pore walls are presented in Fig. 27. The grain size was approximately 1–10 µm. Small wall micropores (less than 1 µm) were visible.

The microporosity improves bone growth into scaffolds. For this purpose the direct foaming method using by polymeric expancel is more appropriated.

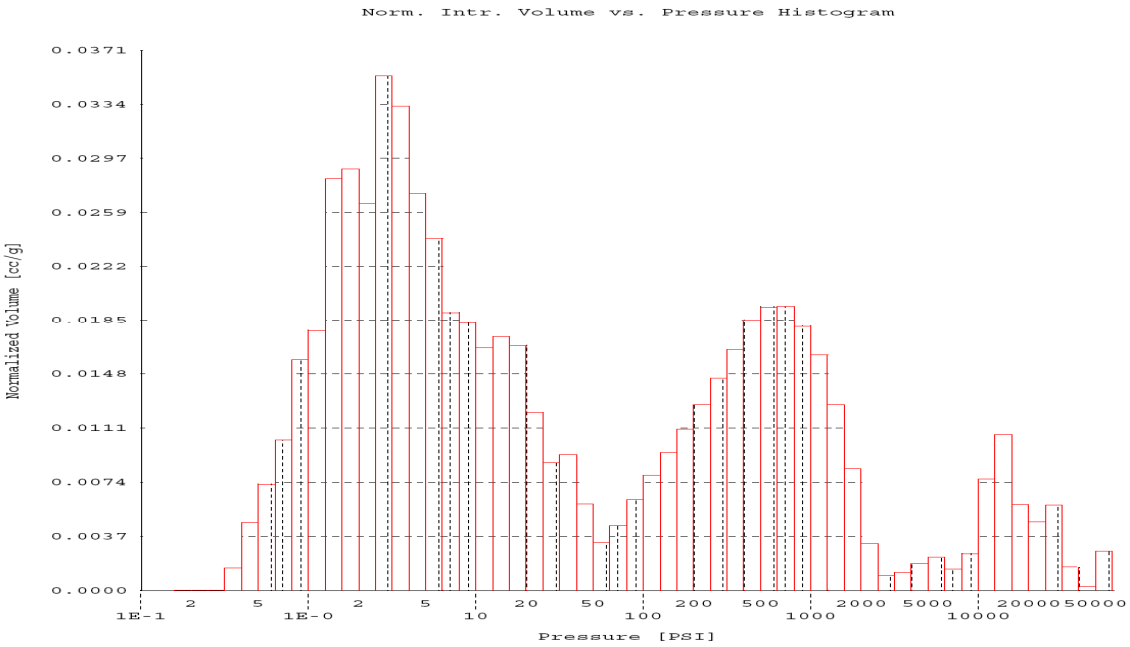

Fig. 28: Applying Hg pressure to normalized volume of pores distribution (precipitation method by polymeric expancel) measered by Hg porosimeter.

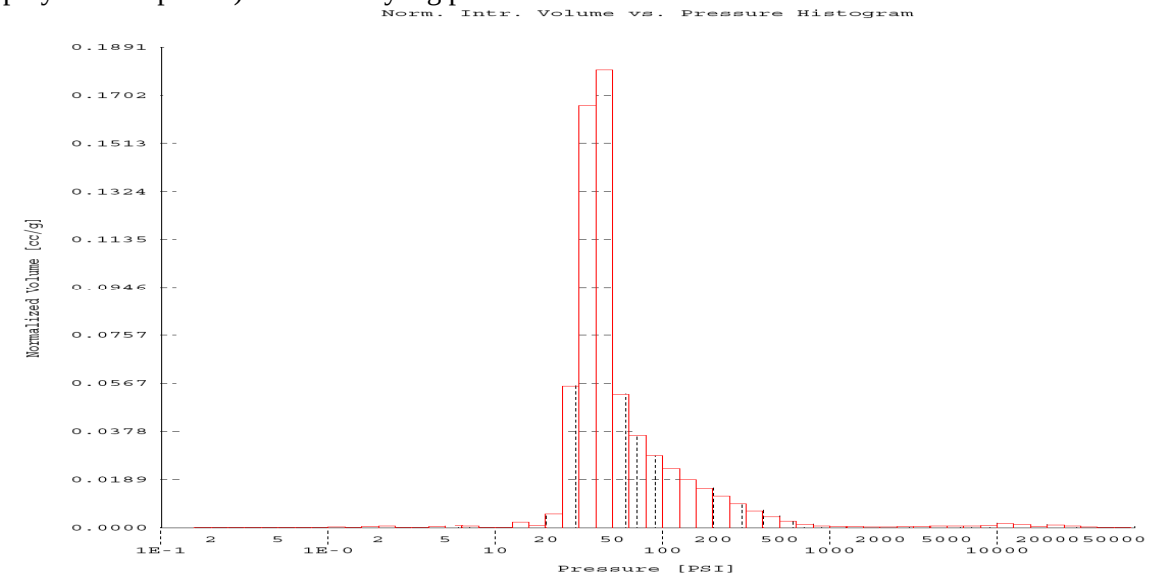

Fig. 29: Applying Hg pressure to normalized volume of pores distribution (sol-gel in ethanol by sponge method) measured by Hg porosimeter.

According to the results of MIP measurements (Figs. 29, 24), the pore structure produced by polymeric sponge method is uniform with single distribution around 50 Psi. One cannot observe the presence of micropores in the samples.

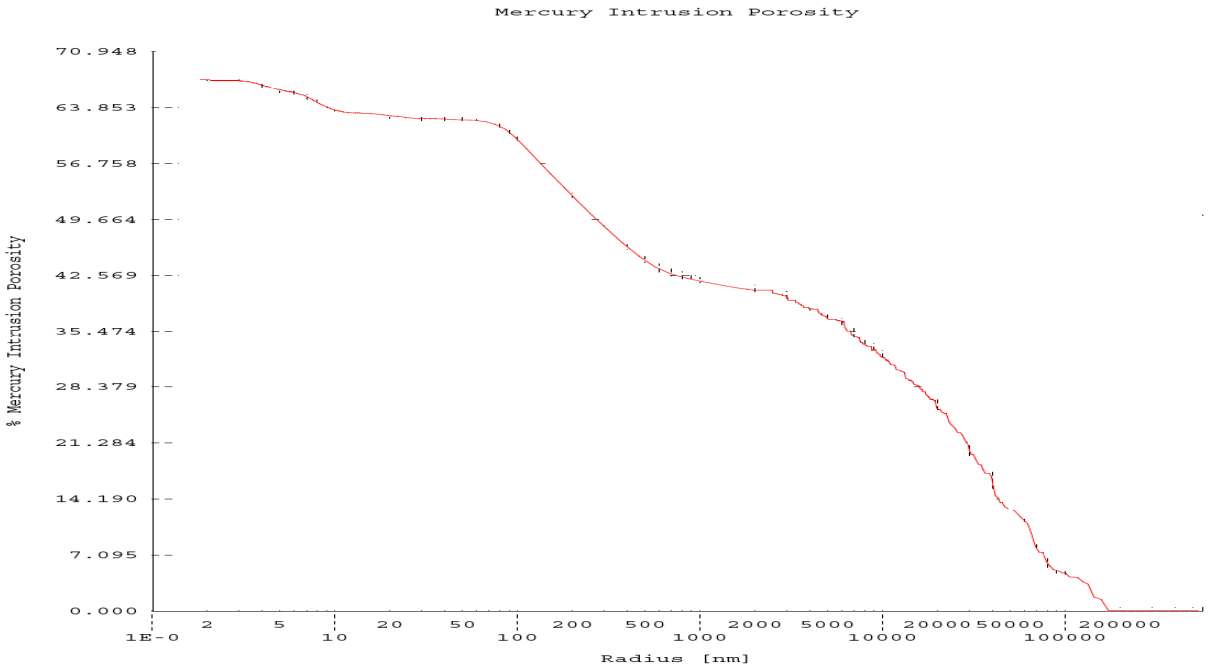

Fig. 30: Pore size distribution curve to Hg Intrusion porosity (%) (precipitation method by polymeric expancel).

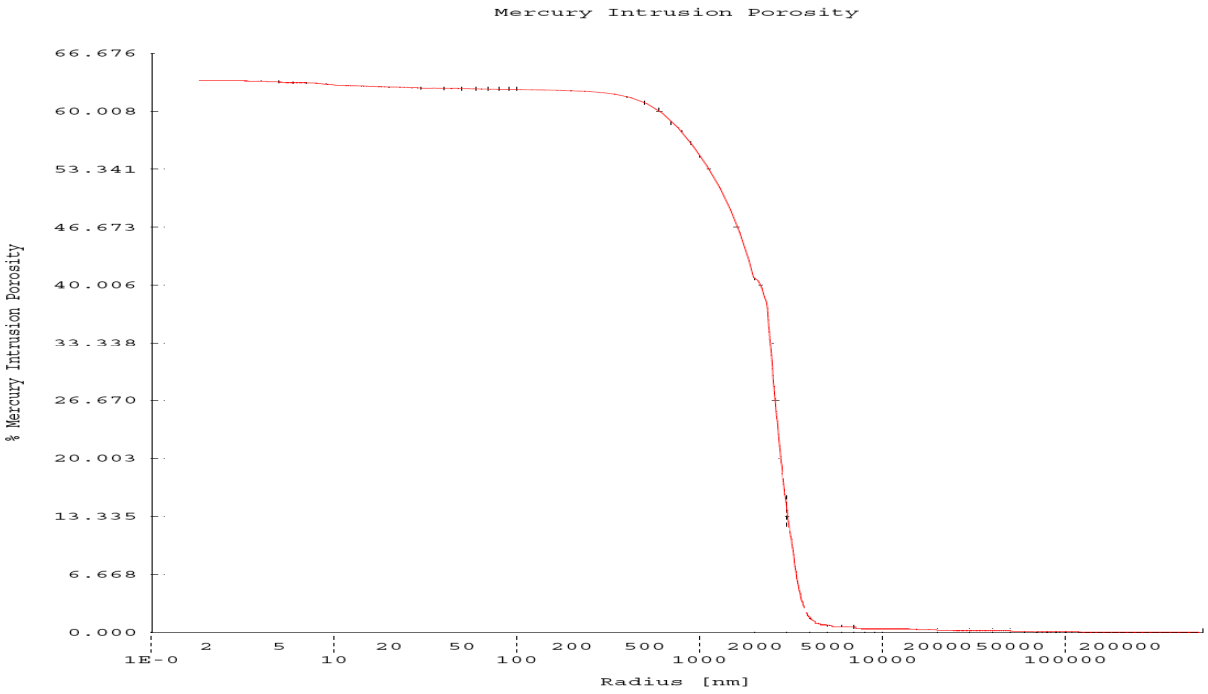

Fig. 31: Pore size distribution curve to Hg Intrusion porosity (%) (sol-gel in ethanol by sponge method).

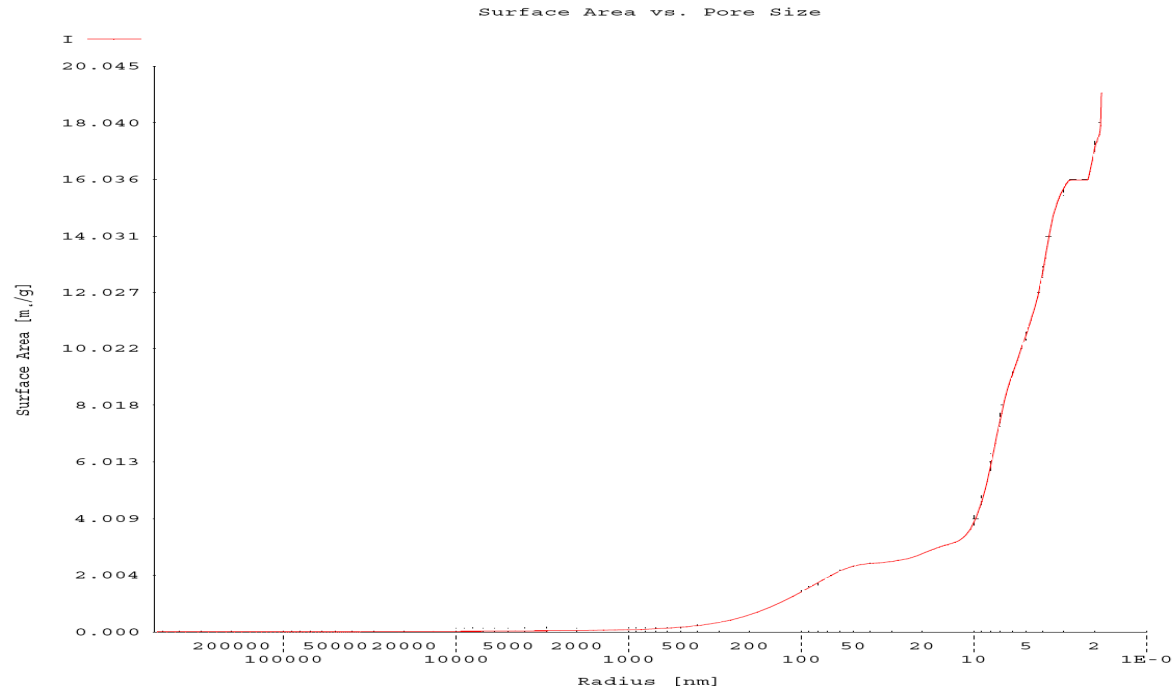

Fig.32: Total surface area to pores distribution (precipitation method by polymeric expancel).

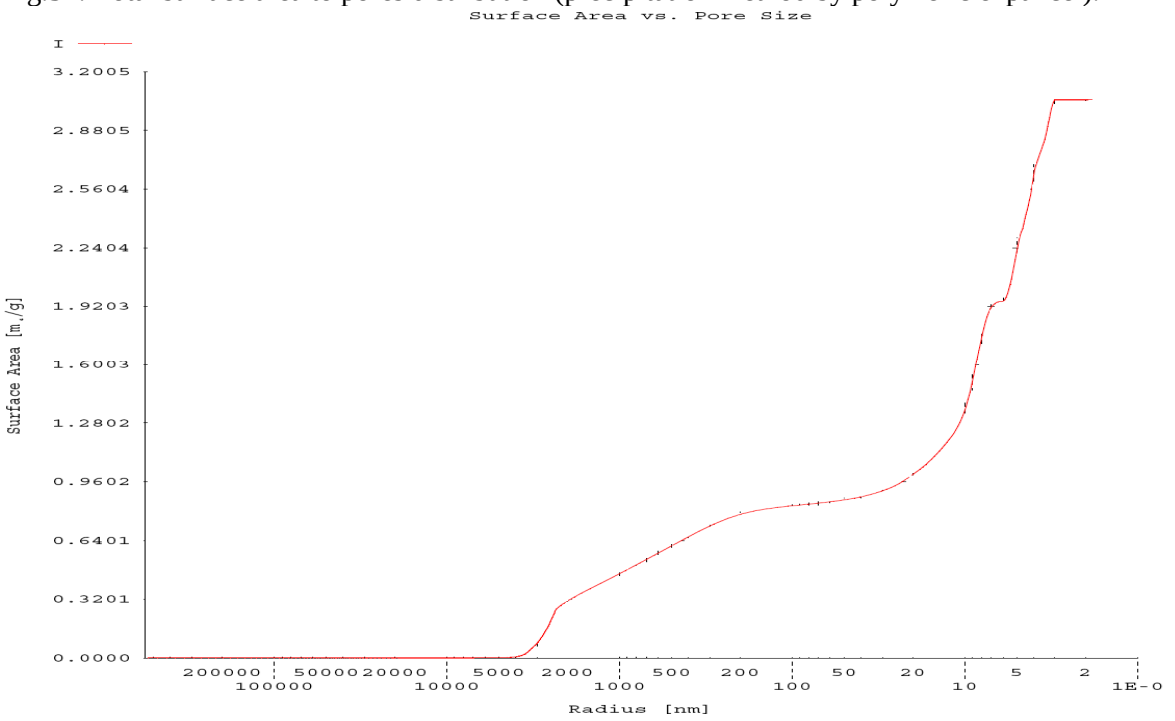

Fig. 33: Total surface area to pores distribution (sol-gel in ethanol by sponge method).

Table 6: Porosity summary by Mercury Intrusion Porosimetry (MIP).

Methods	Direct foaming	Replica technique
Bulk	HAP – precipitate (water)	HAP- Sol-gel (ethanol)
Sample weight (g)	0.087 0	0.188 0
Sample volume (cc)	0.082 0	0.188 3
Total Porosity (%)	67.6	63.5
Theoretical Porosity (%)	46.95	50.08
Total Intruded Volume (cc/g)	0.055 4	0.119 6
Total Surface Area (m/g)	19.090 3	3.048 1
Total Intruded Volume (cc/g)	0.636 9	0.636 0
Intruded volume (interparticle) (cc)	0.033 5	0.080 7
Total interparticle porosity (%)	40.846 0	42.879 2
Intruded volume (intraparticle) (cc)	0.021 9	0.038 8
Total intraparticle porosity (%)	26.7235	20.621 6

Figures 28, 29 represented the histogram of pore size distribution obtained by Mercury Intrusion method (MIP).

The first one, HAP scaffold obtained from direct foaming (measured values in Table 6) and the pore size avoided such as poly-dispersed porosity in the range areas: 50–100 µm, 5–10 µm, 0.5–1 µm.

The second one, HAP scaffold obtained from replica technique (measured values in Table 6) demonstrated the mono-dispersed porosity with the main range area: 0,5–5 µm.

The affection of total porosity and surface area to pore size distribution demonstrate the figures (30, 31, 32, 33).

Therefore scaffold sample prepared from direct foaming required a proper optimization of the processing.

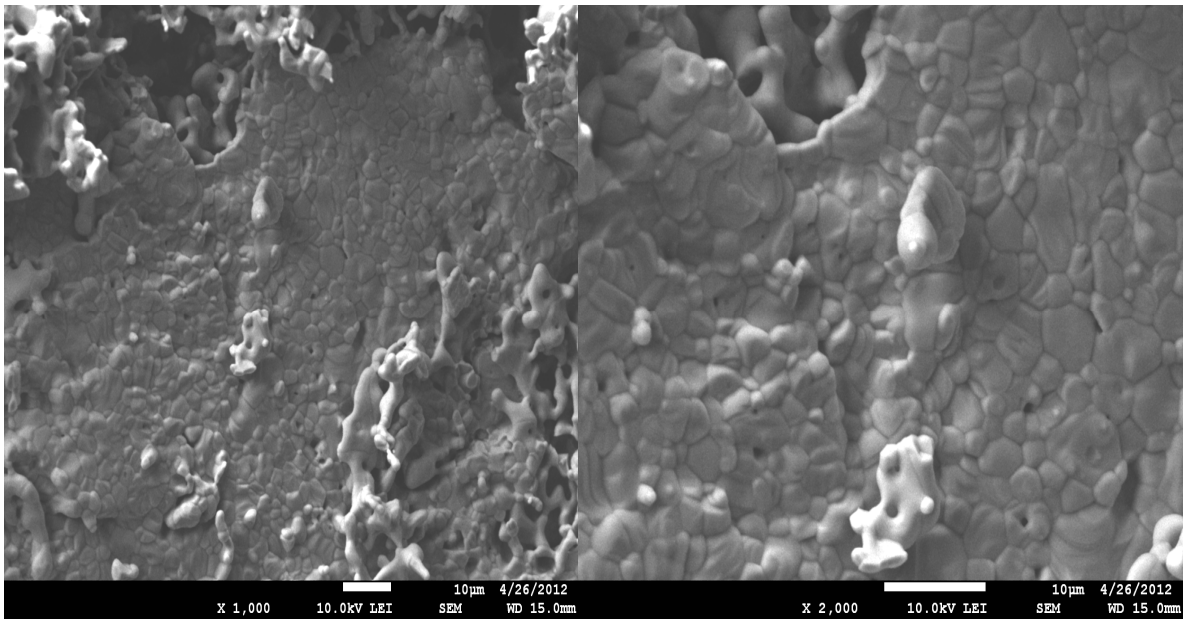

Fig. 34: HAP foaming microstructure after 7 days in SBF (precipitation method by polymeric expancel).

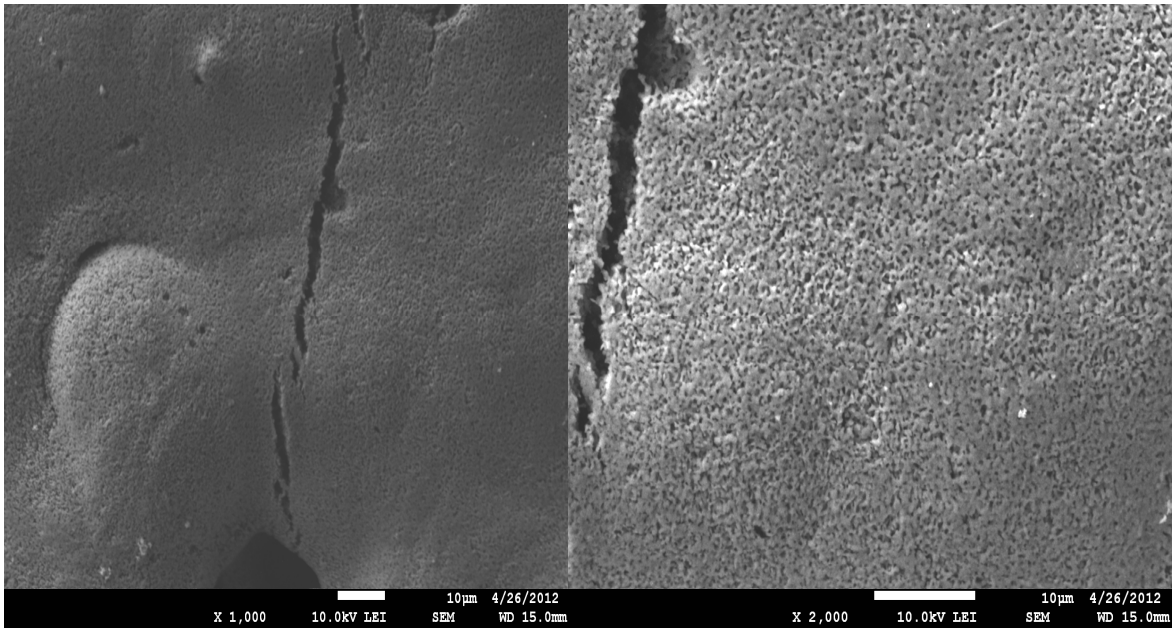

Fig. 35: HAP foaming microstructure after 7 days in SBF (sol-gel in ethanol by sponge method).

The SEM of HAP after being soaked in SBF solution for 7 days is represented by Figures 34 and 35, respectively. The bioactive layer takes place more rapidly in precipitation method due to more porosity gradient and various pores distribution and higher surface area. These aspects are supporting the tissue growing and enhance the bioactivity of porous HAP.

The replica technique enabled us to study more density HAP with regular and one phase porosity which contributes slowly to the tissue growing.

9. CONCLUSION

The goal of diploma work is the synthesis of HAP slurries by different methods following by the study of foaming agent effect on their porosity. The foamed hydroxyaptite ceramics have potential medical application as scaffold for regeneration of damaged tissues. It was shown that ceramic foams can be manufactured by different methods, including replica technique and direct foaming technique, concretely.

The first HAP slurry was made from $Ca(NO_3)_2 \cdot 4H_2O$ and $(NH_4)_2HPO_4$ precursors in higher pH environment of water. The HAP prepared by sol-gel method presents nano scales particles (as be seen in figure 23). The sol-gel method provides uniform particles with homogenity that could support the ossification process than large HAP produced by precipitation method. For this purpose, the sol-gel method is more convenient.

In this way we can prepare the porous HAP using the sponge method (such as replica technique) and polymeric expancel and glass bubbles (such as direct foaming method).

Variety in preparation methods allowed design and production of porous HAP with different parameters.

The microstructure of foamed HAP indicated the micro/meso and macro pore size distribution. The replica technique shows the uniform and fixed pore size and distribution. This HAP porous scaffold should support the cell loading and drug releasing agent.

The direct method showed very diversity microstructure with non-regular pore size and distribution otherwise there is better pores interconnectivity of macro pores in range 400–600 µm and suitable micro pore distribution in range 5–10 µm. This scaffold porosity and pore interconnectivity depended upon the amount of pore former used. The foaming agent is applied for porosity behaviour however it should be used as filler to mechanical strength.

The porous HAP prepared from polymeric sponge method had the total porosity about 63.5 % with surface area 3.084 1 m/g. The pore distribution was mono-phase with range of pore size: 1–5 µm.

The porous HAP prepared by direct foaming agent (polymeric expancel) had the total porosity about 67.6 % with surface area 19.090 3 m/g. The pore distribution was poly-phase with range of pore size: 50–100 µm, 5–10 µm, 0.5–1 µm.

The scaffold and pore size depended on the slurry viscosity and amount of foaming agent and type of replica.

In-*vitro* studies of bioactivity show that rate of tissue growth takes place rapidly in those scaffold which having high porosity and enhance total surface area.

The precipitation method forms likely the new bioactive layers after 7 days in SBF otherwise the sol-gel method by sponge method should soak in SBF more days.

In resulting the preparing porous HAP scaffold is verified as bioactive and it should be utilized in medical application.

10. REFERENCES

[1] BARRÈRE, F., T.A. MAHMOOD, K. DE GROOT a C.A. VAN BLITTERSWIJK. Advanced biomaterials for skeletal tissue regeneration: Instructive and smart functions. *Materials Science and Engineering: R: Reports* [online]. 2008, roč. 59, 1-6, s. 38-71 [cit. 2012-03-12]. ISSN 0927796X. DOI: 10.1016/j.mser.2007.12.001. Dostupné z: http://linkinghub.elsevier.com/retrieve/pii/S0927796X07001234

[2] BASU, Bikramjit, Dhirendra KATTI a Ashok KUMAR. *Advanced biomaterials*: *fundamentals, processing, and applications* [online]. Westerville, Ohio: The American Ceramic Society, c2009, 746 s. [cit. 2012-03-12]. ISBN 04-701-9340-9.

[3] VALLET-REGÍ, María. Evolution of bioceramics within the field of biomaterials. *ComptesRendusChimie* [online]. 2010, roč. 13, 1-2, s. 174-185 [cit. 2012-03-12]. ISSN 16310748. DOI: 10.1016/j.crci.2009.03.004. Dostupné z: http://linkinghub.elsevier.com/retrieve/pii/S1631074809000691

[4] *Biomaterials* [online]. 2003, roč. 24, č. 13 [cit. 2012-03-12]. ISSN 01429612. Dostupné z: http://linkinghub.elsevier.com/retrieve/pii/S0142961203000371

[5] Biomaterials - Classifications and Behaviour of Different Types of Biomaterials. HENESS, G. a BEN-NISSAN. *Www.azom.com* [online]. 2004 [cit. 2012-03-12]. Dostupné z: http://www.azom.com/article.aspx?ArticleID=2630

[6] SLOVIKOVÁ, Alexandra, Lucy VOJTOVÁ a Josef JANČAŘ. Preparation and modification of collagen-based porous scaffold for tissue engineering. *Chemical Papers* [online]. 2008, roč. 62, č. 4, s. 417-422 [cit. 2012-03-12]. ISSN 0366-6352. DOI: 10.2478/s11696-008-0045-8. Dostupné z: http://www.springerlink.com/index/10.2478/s11696-008-0045-8

[7] BEST, S.M., A.E. PORTER, E.S. THIAN a J. HUANG. Bioceramics: Past, present and for the future. *Journal of the European Ceramic Society* [online]. 2008, roč. 28, č. 7, s. 1319-1327 [cit. 2012-03-12]. ISSN 09552219. DOI: 10.1016/j.jeurceramsoc.2007.12.001. Dostupné z: http://linkinghub.elsevier.com/retrieve/pii/S0955221907005961

[8] RIDZWAN, SHUIB, HASSAN a SHOKRI. Problem of stress shielding and Improvement to the Hip Implant designs: A Review. *Journal medical science* [online]. 2007, roč. 7, č. 3 [cit. 2012-03-12]. Dostupné z: http://docsdrive.com/pdfs/ansinet/jms/2007/460-467.pdf

[9] HENCH, L a June WILSON. *An Introduction to bioceramics* [online]. River Edge, N.J.: World Scientific, c1993, 386 s. [cit. 2012-03-12]. ISBN 98-102-1626-2. Dostupné z: http://www.google.cz/books?hl=cs&lr=&id=VRj4lzOYRyMC&oi=fnd&pg=PR7&dq=bioceramic:+Materials+and+Application&ots=ojVA4qYFir&sig=ABbgzH2dnJ46A_7C7P98J1XbLm0&redir_esc=y#v=onepage&q=bioceramic%3A%20Materials%20and%20Application&f=false

[10] NICOLODI, Laura, Emma SJOLANDER a Kristoffer OLSSON. Biocompatible Ceramics - An Overview of Applications and Novel Materials. *Smart Electronic Materials*: *Course 2B1750* [online]. 2004[cit. 2012-03-12]. Dostupné z: http://scholar.google.cz/scholar?q=Biocompatible+Ceramics++An+Overview+of+Applications+and+Novel+Materials&hl=cs&as_sdt=0&as_vis=1&oi=scholart&sa=X&ei=sgxeT8f6DOuO4gSlwvixDw&sqi=2&ved=0CBkQgQMwAA

[11] *Bioceramics*: *properties, characterizations, and applications* [online]. New York: Springer, 2008 [cit. 2012-03-12]. ISBN 03-870-9544-6.

[12] Bioceramics. *Madehow* [online]. [cit. 2012-03-12]. Dostupné z: http://www.madehow.com/Volume-5/Bioceramics.html
[13] Photocatalytic activity of barium and strontium hydroxyapatites. CHIU, Howard a Lim Jia WEI. HWA CHONG INSTITUTION. *Photocatalytic activity of barium and strontium hydroxyapatites* [online]. 2007 [cit. 2012-03-12]. Dostupné z: http://pdc_archive.hci.edu.sg/2007/13-WebReport/Cat-01/1-59/site/bginfo.html
[14] SWAIN, Sanjaya Kumar. *Processing of Porous Hydroxyapatite Scaffold*. Rourkela, 2009. Dostupné z: http://dspace.nitrkl.ac.in/dspace/items-by-author?author=Bhattacharyya%2C+S. MTech Thesis. National Institute of Technology. VedoucípráceDr. S. Bhattacharyya.
[15] MAJLING, Ján; PLESCH, Gustav. Technológia špeciálnýchanorganických materiálov. 2002. Bratislava :Vydavateľstvo STU, 2002. 248 s.
[16] FATHI, M.H. aA. HANIFI. Evaluation and characterization of nanostructure hydroxyapatite powder prepared by simple sol-gel method. *Materials Letters* [online]. 2007, roč. 61, č. 18, s. 3978-3983 [cit. 2012-03-12]. ISSN 0167577X. DOI: 10.1016/j.matlet.2007.01.028. Dostupné z: http://linkinghub.elsevier.com/retrieve/pii/S0167577X0700016X
[17] BOGDANOVICIENE, Irma, Aldona BEGANSKIENE, Kaia TÕNSUAADU, Jochen GLASER, H.-Jürgen MEYER aAivaras KAREIVA. Calcium hydroxyapatite, $Ca_{10}(PO_4)_6(OH)_2$ ceramics prepared by aqueous sol?gel processing. *Materials Research Bulletin* [online]. 2006, roč. 41, č. 9, s. 1754-1762 [cit. 2012-03-12]. ISSN 00255408. DOI: 10.1016/j.materresbull.2006.02.016. Dostupné z: http://linkinghub.elsevier.com/retrieve/pii/S0025540806000778
[18] RAMANAN, Sutapa Roy a Ramanan VENKATESH. A study of hydroxyapatite fibers prepared via sol-gel route. *Materials Letters* [online]. 2004, roč. 58, č. 26, s. 3320-3323 [cit. 2012-03-12]. ISSN 0167577X. DOI: 10.1016/j.matlet.2004.06.030. Dostupné z: http://linkinghub.elsevier.com/retrieve/pii/S0167577X04004355
[19] BRINKER, C a George W SCHERER. *Sol-gel science*: *the physics and chemistry of sol-gel processing* [online]. Boston: Academic Press, c1990, 908 s. [cit. 2012-03-12]. ISBN 01-213-4970-5
[20] GOMES, Paulo J., Viviana M. T. M. SILVA, Paulo A. QUADROS, Madalena M. DIAS a LOPES. A Highly Reproducible Continuous Process for Hydroxyapatite Nanoparticles Synthesis. *Journal of Nanoscience and Nanotechnology* [online]. 2009-06-01, roč. 9, č. 6, s. 3387-3395 [cit. 2012-03-15]. ISSN 15334880. DOI: 10.1166/jnn.2009.NS06.
[21] LARANJEIRA, Paulo E., António A. MARTINS, Maria Isabel NUNES, José Carlos B. LOPES a Madalena M. DIAS. NETmix®, a new type of static mixer: Experimental characterization and model validation. *AIChE Journal* [online]. 2011, roč. 57, č. 4, s. 1020-1032 [cit. 2012-03-15]. ISSN 00011541. DOI: 10.1002/aic.12316. Dostupné z: http://doi.wiley.com/10.1002/aic.12316
[22] Groeneveld E.H, Van den Bergh J.P, Holzmann P, Ten Bruggenkate C.M, Tuinzing D.B, Burger E.H. Mineralization processes in de-mineralized bone matrix grafts in human maxillary sinus floor elevations. J BiomedMater Res 1999; 48(4):393–402
[23] SÁNCHEZ-SALCEDO, S., A. NIETO a M. VALLET-REGÍ. Hydroxyapatite/?-tricalcium phosphate/agarose macroporous scaffolds for bone tissue engineering. [online]. [cit. 2012-03-19]. DOI: 10.1016/j.cej.2007.09.011. Dostupné z: http://linkinghub.elsevier.com/retrieve/pii/S1385894707006183

[24] Hulbert S.F, Young F.A, Mathews R.S, Klawitter J.J,Talbert C.D, Stelling F.H. Potential of ceramic materials as permanently implantable skeletal prostheses. J BiomedMater Res 1970;4(3):433–56
[25] Leony Leon C.A.New perspectives in mercury porosimetry. Adv Colloid Interface Sci 1998;76–77:341–72.
[26] Itala AI, Ylanen H.O, Ekholm C, Karlsson K.H, Aro H.T. Pore diameter of more than 100 micron is not requisite for bone ingrowth in rabbits. J BiomedMater Res 2001;58(6):679–83
[27] STUDART, Andre R., Urs T. GONZENBACH, Elena TERVOORT a Ludwig J. GAUCKLER. Processing Routes to Macroporous Ceramics: A Review. *Journal of the American Ceramic Society* [online]. 2006, roč. 89, č. 6, s. 1771-1789 [cit. 2012-04-02]. ISSN 0002-7820. DOI: 10.1111/j.1551-2916.2006.01044.x. Dostupné z: http://doi.wiley.com/10.1111/j.1551-2916.2006.01044.x
[28] POTOCZEK, Marek, Aneta ZIMA, Zofia PASZKIEWICZ a Anna ŚLÓSARCZYK. Manufacturing of highly porous calcium phosphate bioceramics via gel-casting using agarose. [online]. [cit. 2012-03-19]. DOI: 10.1016/j.ceramint.2008.12.006. Dostupné z: http://linkinghub.elsevier.com/retrieve/pii/S0272884209000297
[29] SOPYAN, I., M. MEL, S. RAMESH a K.A. KHALID. Porous hydroxyapatite for artificial bone applications. [online]. [cit. 2012-03-19]. DOI: 10.1016/j.stam.2006.11.017. Dostupné z: http://stacks.iop.org/1468-6996/8/i=1-2/a=A21?key=crossref.4412a0f22a4464474c8a5a963155a75c
[30] ZESCHKY, J. Preceramic polymer derived cellular ceramics. [online]. [cit. 2012-03-19]. DOI: 10.1016/S0266-3538(03)00269-0. Dostupné z: http://linkinghub.elsevier.com/retrieve/pii/S0266353803002690
[31] JONES, Julian R a HENCH. Regeneration of trabecular bone using porous ceramics. [online]. [cit. 2012-03-19]. DOI: 10.1016/j.cossms.2003.09.012. Dostupné z: http://linkinghub.elsevier.com/retrieve/pii/S1359028603000767
[32] LUYTEN, J., S. MULLENS, J. COOYMANS, A.M. DE WILDE, I. THIJS a R. KEMPS. Different methods to synthesize ceramic foams. [online]. [cit. 2012-03-19]. DOI: 10.1016/j.jeurceramsoc.2008.07.039. Dostupné z: http://linkinghub.elsevier.com/retrieve/pii/S0955221908003725
[33] DRESSLER, M., F. DOMBROWSKI, U. SIMON, J. BÖRNSTEIN, V.D. HODOROABA, M. FEIGL, S. GRUNOW, R. GILDENHAAR a M. NEUMANN. Influence of gelatin coatings on compressive strength of porous hydroxyapatite ceramics. *Journal of the European Ceramic Society* [online]. 2011, roč. 31, č. 4, s. 523-529 [cit. 2012-04-23]. ISSN 09552219. DOI: 10.1016/j.jeurceramsoc.2010.11.004. Dostupné z: http://linkinghub.elsevier.com/retrieve/pii/S0955221910005091
[34] Lead in the human femoral head:Relationships of pathology, environmental exposure, micro-architecture, and biocultural contributions to bone quality. *Grin* [online]. [cit. 2012-04-02]. Dostupné z: http://www.grin.com/en/doc/252785/lead-in-the-human-femoral-head-relationships-of-pathology-environmental
[35] Sol-gel technology. *Chemat technology* [online]. [cit. 2012-04-02]. Dostupné z: http://www.chemat.com/chemattechnology/SolGel.aspx

[36] KURIAKOSE, T.Anee, S.Narayana KALKURA, M. PALANICHAMY, D. ARIVUOLI, Karsten DIERKS, G. BOCELLI a C. BETZEL. Synthesis of stoichiometric nano crystalline hydroxyapatite by ethanol-based sol?gel technique at low temperature. *Journal of Crystal Growth* [online]. 2004, roč. 263, 1-4, s. 517-523 [cit. 2012-04-02]. ISSN 00220248. DOI: 10.1016/j.jcrysgro.2003.11.057.

[37] Precipitation (chemistry). *Wikipedia.org* [online]. 2012 [cit. 2012-04-22]. Dostupné z: http://en.wikipedia.org/wiki/Precipitation_%28chemistry%29

[38] AKZONOBEL. *Expancel microspheres a technical presentation*. Sweden, 2006. Dostupné z: www.expancel.com

[39] Sintering of ceramics. KOPELIOVICH, Dmitri. *Substances&technologies* [online]. 2010 [cit. 2012-04-21]. Dostupné z: http://www.substech.com/dokuwiki/doku.php?id=sintering_of_ceramics

[40] FATHI, M.H., A. HANIFI a A. LERICHE. Evaluation and characterization of nanostructure hydroxyapatite powder prepared by simple sol-gel method. *Materials Letters* [online]. 2007, roč. 61, č. 18, s. 3978-3983 [cit. 2012-04-21]. ISSN 0167577x. DOI: 10.1016/j.matlet.2007.01.028. Dostupné z: http://linkinghub.elsevier.com/retrieve/pii/S0167577X0700016X

[41] Ohtsuki C, KokuboT, YamamuroT. “Mechanism of HA formation of CaO-SiO2-P2O5 glasses in simulated body fluid”. J Non- Cryst Solids 1992; 143:84-92.

[42] PRAMANIK, Sumit, et al. Development of high strength hydroxyapatite by. *Ceramics International* [online]. 2007, 33, 3, [cit. 2010-05-12]. Dostupný z WWW: <www.sciencedirect.com>.

[43] Hyun-Min Kima, Teruyuki Himeno, Tadashi Kokubo, Takashi Nakamura; “Process and kinetics of bonelike apatite formation on sintered hydroxyapatite in a simulated body fluid” Biomaterials 26 (2005) 4366–4373.

[44] X-ray Powder Diffraction (XRD). *Skip to navigation Geochemical Instrumentation and Analysis* [online]. 2012 [cit. 2012-04-21]. Dostupné z: http://serc.carleton.edu/research_education/geochemsheets/techniques/XRD.html

[45] Infrared spectroscopy. *Wikipedia* [online]. 2012 [cit. 2012-04-21]. Dostupné z: http://en.wikipedia.org/wiki/Infrared_spectroscopy

[46] Scanning electron microscope. *Wikipedia* [online]. 2012 [cit. 2012-04-21]. Dostupné z: http://en.wikipedia.org/wiki/Scanning_electron_microscope

[47] SPECIAL SECTION/INSTRUMENTATION: Mercury Intrusion Porosimetry. DESOUSA, Trish. *Ceramic industry* [online]. 2010 [cit. 2012-04-21]. Dostupné z: http://www.ceramicindustry.com/articles/special-section-instrumentation-mercury-intrusion-porosimetry

[48] DESCAMPS, M., J.C. HORNEZ a A. LERICHE. Effects of powder stoichiometry on the sintering of β -tricalcium phosphate. *Journal of the European Ceramic Society* [online]. 2007, roč. 27, č. 6, s. 2401-2406 [cit. 2012-04-21]. ISSN 09552219. DOI: 10.1016/j.jeurceramsoc.2006.09.005.

[49] BIOGRAFT - Synthetic Hydroxyapatite and beta tricalcium phosphate promising bio materials especially in the orthopaedic and dental fields. [online]. [cit. 2012-04-21]. Dostupné z: http://www.ifglbioceramics.com/ifglbioceramics/download/dr_g_banarjee.doc

[50] 3M COMPANY. *3M Scotchlite Glass bubbles*. United States, 2003. Dostupné z: www.3m.com/microspheres.

[51] NICOLODI, Laura, Emma SJOLANDER a Kristoffer OLSSON. Biocompatible Ceramics - An Overview of Applications and Novel Materials. *Smart Electronic materials*: *Course 2B1750* [online]. 2004 [cit. 2012-04-23].

LIST OF SYMBOLS

UHMWPE	Ultra high molecular weight polyethylene
PMMA	Polymethylmethacrylate
TZP	Tetragona zirconium oxide–polycrystalic
DL-PLA	Dilactic-polyactic acid
Ca/P	Calcium/Phosphate
HAP	Hydroxyapatite
SBF	Simulated body fluid
ACP	Apatite calcium phosphate
BCP	Biphasic calcium phosphate
TCP	Tri calcium phosphate
A/W	Apatite–wollastonite
SEM	Scanning electrone microscope
XRD	X-ray diffraction
FTIR	Fourier transformed infrared spectrometer
MIP	Mercury Intrusion porisimetry